Prominin-1 Is a Novel Regulator of Autophagy in the Human Retinal Pigment Epithelium

Sujoy Bhattacharya,[1] Jinggang Yin,[1] Christina S. Winborn,[1] Qiuhua Zhang,[1] Junming Yue,[2] and Edward Chaum[1,3]

[1]Department of Ophthalmology, University of Tennessee Health Science Center, Memphis, Tennessee, United States
[2]Department of Pathology, University of Tennessee Health Science Center, Memphis, Tennessee, United States
[3]Department of Anatomy and Neurobiology, University of Tennessee Health Science Center, Memphis, Tennessee, United States

Correspondence: Edward Chaum, Plough Foundation Professor of Retinal Diseases, UTHSC Hamilton Eye Institute, 930 Madison Avenue, Memphis, TN 38163, USA; echaum@uthsc.edu.

Submitted: November 22, 2016
Accepted: March 21, 2017

Citation: Bhattacharya S, Yin J, Winborn CS, Zhang Q, Yue J, Chaum E. Prominin-1 is a novel regulator of autophagy in the human retinal pigment epithelium. *Invest Ophthalmol Vis Sci*. 2017;58:2366–2387. DOI: 10.1167/iovs.16-21162

Purpose. Prominin-1 (Prom1) is a transmembrane glycoprotein, which is expressed in stem cell lineages, and has recently been implicated in cancer stem cell survival. Mutations in the Prom1 gene have been shown to disrupt photoreceptor disk morphogenesis and cause an autosomal dominant form of Stargardt-like macular dystrophy (STGD4). Despite the apparent structural role of Prom1 in photoreceptors, its role in other cells of the retina is unknown. The purpose of this study is to investigate the role of Prom1 in the highly metabolically active cells of the retinal pigment epithelium (RPE).

Methods. Lentiviral siRNA and the genome editing CRISPR/Cas9 system were used to knockout Prom1 in primary RPE and ARPE-19 cells, respectively. Western blotting, confocal microscopy, and flow sight imaging cytometry assays were used to quantify autophagy flux. Immunoprecipitation was used to detect Prom1 interacting proteins.

Results. Our studies demonstrate that Prom1 is primarily a cytosolic protein in the RPE. Stress signals and physiological aging robustly increase autophagy with concomitant upregulation of Prom1 expression. Knockout of Prom1 increased mTORC1 and mTORC2 signaling, decreased autophagosome trafficking to the lysosome, increased p62 accumulation, and inhibited autophagic puncta induced by activators of autophagy. Conversely, ectopic overexpression of Prom1 inhibited mTORC1 and mTORC2 activities, and potentiated autophagy flux. Through interactions with p62 and HDAC6, Prom1 regulates autophagosome maturation and trafficking, suggesting a new cytoplasmic role of Prom1 in RPE function.

Conclusions. Our results demonstrate that Prom1 plays a key role in the regulation of autophagy via upstream suppression of mTOR signaling and also acting as a component of a macromolecular scaffold involving p62 and HDAC6.

Keywords: CD133, Atg5, Atg7, LC3-II, Akt, p62, mTORC1, mTORC2, autophagy flux, Nutlin-3

Prominin-1 (Prom1), also known as CD133, is a membrane glycoprotein with five membrane-spanning domains, two large N-glycosylated extracellular loops, and an intracellular C-terminus.[1] Human CD133 (encoded by the PROM1 gene) was cloned from the WERI-Rb-1 retinoblastoma cell line[2,3] and contains 37 exons located in the chromosomal region 4p 15.32.[4] Prom1 is best known as a stem cell marker,[5,6] and its glycosylated epitope, AC133, has been widely used as a marker of cancer stem cells in many human malignancies,[7] but its expression includes endothelial progenitor cells and some terminally differentiated cells.[4,6] Prom1 has been primarily characterized as an organizer of the plasma membrane because of its: (1) localization at plasma membrane protrusions such as filopodia and lamellipodia;[8] (2) enrichment in cholesterol-rich membrane microdomains;[9,10] (3) association with membrane-particles (known as prominosomes);[1] and (4) association with apical microvilli and microvilli-related structures in various epithelia of the mouse embryo.[11] In addition to maintaining membrane protrusions, recent studies demonstrated translocation of CD133 from membrane to cytoplasm in response to low-glucose medium[12] and trafficking of Prom1 to the lysosomes via physical interactions between Prom1 and cytosolic histone deacetylase 6 (HDAC6),[13] suggesting a role of Prom1 in the lysosomal-endosomal and autophagy pathways.

In the visual system, Prom1 is concentrated in the photoreceptor outer segment disc membranes and is thought to play a structural role.[14] A study of Prom1$^{-/-}$ mice showed Prom1 to be required for retinal development and photoreceptor disk morphogenesis.[8] Expression of the human dominant Prom1 R373C mutation in mice disrupted photoreceptor disk morphogenesis, suggesting that Prom1 plays an integral role in the structural organization of the outer segment.[14] Retinal degeneration has been reported in a spontaneous knock out mouse (Prom1^{rd19}) carrying a point mutation in the Prom1 gene.[15] Human mutations in the Prom1 gene cause Stargardt-like and bull's eye macular dystrophies[16] and retinitis pigmentosa.[17] The RPE performs many functions that maintain the health of the overlying photoreceptors. One critical function performed by the RPE is the phagocytosis and lysosomal degradation of shed photoreceptor outer segment tips.[18] Recent studies have shown that autophagy by the RPE is fundamental to this activity.[19,20]

Autophagy is an evolutionarily conserved intracellular housekeeping process that provides an essential mechanism

for removing damaged organelles and misfolded protein aggregates within the cell. Autophagy can be categorized into chaperone-mediated microautophagy and a catabolic macroautophagy involving bulk lysosomal degradation of organelles and macromolecules.[21,22] The selective autophagy receptor, p62/SQSTM1 (hereafter referred to as p62), acts as a signaling hub by shuttling ubiquitinated protein cargoes to the autophagosome and transporting misfolded proteins to the lysosome for their degradation.[23] Autophagy is comprised of sequential steps including autophagosome initiation, elongation, and its maturation through fusion with lysosomes, which require a family of autophagy-related genes (*Atg*). Upstream of Atg proteins, mammalian target of rapamycin (mTOR) is an atypical serine/threonine protein kinase that serves as a central convergence point for diverse stimuli involved in cell metabolism, proliferation, and survival. mTOR belongs to the phosphatidylinositol 3-kinase related kinase (PIKK) family and plays diverse roles through participation in two protein complexes referred to as mTOR complex 1 (mTORC1) and mTOR complex 2 (mTORC2). Under sufficient supply of nutrients, the rapamycin (RAP) sensitive mTORC1 promotes cell growth by directly phosphorylating S6 kinase 1,[24] and inhibits autophagy by preventing ULK1 activation by phosphorylating ULK1 at Ser757.[25] The RAP insensitive mTORC2 directly activates its downstream target Akt by phosphorylating Ser473.[26] Thus, multiple signaling cascades coupled with concerted action of specific upstream molecules tightly regulate autophagy.

Induction of autophagy has been shown to protect the RPE from lipofuscin accumulation[27] and protect against photoreceptor cell death.[28] Impairment in any step of autophagosome maturation or delayed trafficking of autophagosomes with the lysosomes can disrupt the effective clearing of intracellular debris, thereby contributing to the build-up of toxic waste in the cell. Decreased rates of autophagy have been implicated in the pathogenesis of neurodegenerative diseases,[29] and impairment of autophagy has been shown to increase susceptibility to age-related macular degeneration (AMD).[27]

In this study, we investigated the functional role and significance of Prom1 in the RPE. Using a lentiviral construct overexpressing Prom1 and CRISPR/Cas9 knockout (KO) of Prom1 in the RPE, we demonstrate that Prom1 is a novel and key regulator of autophagosome formation and turnover. Our data reveal a molecular mechanism by which Prom1 regulates autophagy flux in the RPE via p62 and HDAC6 association, and by its ability to inhibit mTORC1 and mTORC2 activities.

Methods

Reagents

Disposable cell culture ware was purchased commercially (Corning Glass Works, Corning, NY, USA). The ARPE-19 cell line was purchased from ATCC CRL-2302 (Manassas, VA, USA), and the human retinal endothelial cell (HREC) line was a kind gift from Jena Steinle. Cell culture medium was obtained from Lonza (Walkersville, MD, USA), and fetal bovine serum (FBS) was purchased from Atlanta Biologicals (Flowery Branch, GA, USA). Other materials, purchased commercially, were: permeable supports (Transwell; Corning, Lowell, MA, USA); enhanced chemiluminescence (ECL) western blot detection system (Perkin Elmer, Inc., Boston, MA, USA); cleaved active caspase-3 (Asp 175); LC3-I/LC3-II; SQSTM1/p62, phospho-p62 Ser349, Atg5, Atg7, Atg3, p-Akt Ser 473, total-Akt, HDAC-6, GFP, and phospho-S6 Ribosomal protein Ser235/236 antibodies (Cell Signaling Technology, Inc., Beverly, MA, USA); HIF-1 α antibody (Novus Biologicals, Littleton, CO, USA); rabbit polyclonal Prom1 antibody (OriGene, Rockville, MD, USA, and Aviva Systems Biology Corp., San Diego, CA, USA); anti-mouse Prom1/CD133 antibodies (Miltenyi Biotec, Auburn, CA, USA, and GeneTex, Inc., Irvine, CA, USA); Zonula Occludens (ZO-1) and β-catenin antibodies (Zymed Laboratories, South San Francisco, CA, USA); Alexa-Fluor 488 conjugated, Alexa-Fluor 647, and Cy3 conjugated secondary antibodies (Molecular Probes, Eugene, OR, USA); RAP, Bafilomycin A1 (BAF), and Torin-1 (EMD Biosciences/Millipore Corp., Billerica, MA, USA); Torin-2 (Tocris Bioscience, Avonmouth, Bristol, UK); Chloroquine (CQ) and Lysotracker (Invitrogen, Thermo Fisher Scientific, Waltham, MA, USA); Nutlin-3 and Earle's Balanced Salt Solution (EBSS; Sigma-Aldrich Corp., St. Louis, MO, USA). All chemicals were of the highest purity commercially available.

Prom1 Gene Targeting by siRNA

Lentiviral vectors containing human Prom1 siRNA (piLenti-Prom1-siRNA-GFP) were purchased from Applied Biological Materials, Inc. (Richmond, Canada). A dual convergent promoter system where two different promoters (U6 and H1 promoters) controlled the sense and antisense strands of the siRNA was used. Four siRNA lentiviral constructs (Prom1-603-siRNA, Prom1-736-siRNA, Prom1-1087-siRNA, Prom1-1270-siRNA) were used to knock down Prom1 expression in RPE cells. Four constructs were transfected in primary RPE cells using Fugene-6 HD. GFP expression by live cell confocal microscopy was used to monitor transfection efficiency. Forty-eight hours posttransfection, RPE cells were treated with puromycin to enrich cultures expressing Prom1 siRNA. GFP-positive stable transfectants with puromycin resistance were used for further analyses. Western blotting with Prom1 antibody was used to evaluate Prom1 expression in cells stably transfected with lentiviral-siRNA.

Confocal Microscopy

Confluent RPE and HREC cell monolayers were fixed in ice-cold Acetone/Methanol (1:1) followed by permeabilization in 0.1% Triton X-100. After permeabilization, the monolayers were blocked in 5% BSA in PBS and further incubated with primary antibodies (rabbit polyclonal Prom1, mouse β-catenin, rabbit LC3-I and LC3-II) for 1 hour at 37°C, followed by 1 hour incubation with secondary antibodies (Alexa Fluor 488-conjugated anti-mouse IgG and Cy-3 conjugated anti-rabbit IgG antibodies). For LC3 staining, cells were mounted on glass slides using mounting medium containing 4′,6-diamidino-2-phenylindole (DAPI). For localization of Prom1 and β-catenin, the fluorescence was examined under a Zeiss LSM 5 laser scanner confocal microscope, and images were collected using LSM 5 Pascal software as described earlier. Images were stacked using the software, Image J (National Institutes of Health, Bethesda, MD, USA), and processed by Adobe Photoshop (Adobe Systems, Inc., San Jose, CA, USA).

Prom1 Lentiviral Construct

The wild-type (WT) Prom1 lentiviral construct (pLenti-GIII-CMV-GFP-2A-Puro; (NM_001145848.1) was obtained from Applied Biological Materials, Inc., expressing Prom1 under the control of CMV promoter. Plasmids were amplified using the Qiagen Plasmid maxi prep kit following the manufacturers instructions. Ten micrograms Prom1 plasmid and the empty GFP control plasmid were packaged in human 293FT cells and purified through ultracentrifugation at the Viral Vector Core laboratory as described previously.[30]

CRISPR-Cas9-Mediated Genomic Deletion of Prom1

The 17-nucleotide guide RNA (gRNA) sequence (5′-GGATG CACCAAGCACAG- 3′) was used to target human PROM1 gene at exon 10. Oligonucleotides were purchased from Integrated DNA technology and annealed, followed by phosphorylation through T4 DNA polynucleotide kinase reaction. The annealed double-stranded DNA was cloned into the BsmBI–BsmBI sites downstream from the human U6 promoter in the Lenti-CRISPR v2 plasmid (Addgene plasmid #52961). The Lenti-CRISPR-Prom1 construct was packaged into 293FT cells and purified as described previously.[30] Purified lentivirus was used to infect ARPE-19 cells. During infection, 15 μL of the purified lentivirus (Cas9 or Prom1-Cas9) was added to 60% to 70% confluent monolayers in a six-well plate with 4 μg/mL polybrene and incubated at 37°C for 48 hours. The virus containing culture medium was removed and replaced with 2 mL complete medium. Cells were allowed to recover overnight, followed by passaging of cells and selection of stable lines with 1.5 μg/mL puromycin for 48 hours. Puromycin-resistant cells were expanded in culture, cloned, and subsequently used for autophagy experiments.

Genomic DNA Analysis

Overexpression and KO of Prom1 were verified by genomic DNA analysis. Control ARPE-19 cells, and cells infected with empty Cas9, WT Prom1, and CRISPR Cas9 lentivirus were used to extract genomic DNA using the QIAamp DNA micro kit. PCR was performed using the forward primer: 5′-TAGTTGGAGCAGCTGTTAGAGCA-3′ and reverse primer: 5′-ATGGTGATCAAATGACTCAAGAAG-3′. The single band PCR product was confirmed using a 1.2% agarose gel for each cell line. The PCR products were purified with the QIA quick PCR Purification kit and quantified by Nano Drop Spectrophotometry. The purified PCR products were inserted into the pCR2.1 vector using the TA Cloning kit (Invitrogen). For each reaction, 100 ng PCR product, 12.5 ng pCR2.1 vector, 2.5 U Express Link T4 DNA Ligase, and 2 μL 5X T4 DNA ligase reaction buffer were mixed in a total reaction volume of 10 μL at room temperature for 1 hour. Immediately after incubation, an aliquot (50 μL) of DH5-α was gently added to the mix and kept on ice for 30 minutes, followed by heat shock for 45 seconds at 42°C. The mix was subsequently transferred on ice for 2 minutes followed by the addition of 0.5 mL NZY broth. The contents were subsequently incubated at 37°C for 1 hour with shaking at 225 rpm. Aliquots of 250 μL from each reaction mixture were transferred on LB-ampicillin agar plates containing 80 μg/mL X-gal and 20 mM IPTG. Plates were incubated at 37°C for 16 hours, and five white colonies were picked from each reaction for extraction and amplification of the plasmid. Each plasmid sample was digested by EcoRI and analyzed on a 1.2% agarose gel. The double bands in the agarose gel were sequenced using the M13 reverse primer. Genomic sequences were BLAST analyzed to confirm the WT and different KO sequences. Sequence analyses revealed a Prom1-KO ARPE-19 line with one base pair (bp) insertion, and several other lines with multiple bp deletions. The original Prom1-KO line was cloned, and both KO and clone-6 were used for our experiments.

KO: TTGATGGATGCACCAAG————AGGGTCATTGAGA GATGACCGCAGGCT
KO-clone6: TTGATGGATGCACCAAGCAACAGAGGGTCATT GAGAGATGACCGCAGGCT
WT: TTGATGGATGCACCAAGCA-CAGAGGGTCATTGAGA GATGACCGCAGGCT

Real-Time PCR

TRIzol reagent (Thermo Fisher Scientific) was used to extract total RNA from cells infected with Cas9 and Cas9-Prom1 lentivirus. Total RNA concentrations were quantified by measuring A_{260} and A_{280} using NanoDrop spectrophotometry. Total RNA (1 μg) was reverse transcribed to cDNA using a kit from Promega (Madison, WI, USA) and following the manufacturer's instructions. The cDNA was diluted 1:5 with DNase-free water. Real-time qPCR was performed using an ABI PRISM 7700 Sequence Detection System (Applied Biosystems, Foster City, CA, USA) with 2.5 μL cDNA product in a 25-μL reaction mixture containing 1X SYBR Green master mix (Applied Biosystems) and 120 nM forward and reverse primers. The primers used for PROM1 (forward 5′-TCAATGACCCTCTGTGCTTG-3′) CTGTGCTTG of the forward sequence from gsRNA sequence (5′-CAAGCACAG-3′), reverse: 5′-AAGACGCTGAGTTACATTG TCG-3′; FBJ murine osteosarcoma viral oncogene homolog B (*FOSB*): forward, 5′-GTGTGAGCGCTTCTGCAGC-3′, reverse, 5′-CCA ATT CAA CGG CTC GCT T-3′ sequences were used. The qPCR conditions were 50°C for 2 minutes, 95°C for 10 minutes, followed by 40 cycles of 95°C for 15 seconds and 60°C for 1 minute, as described previously.[31] Each reaction was performed in triplicate.

Real-time RT-PCR was used to detect various regions of Prom1 mRNA transcript variant 3 (NM_001145848.1) in control ARPE-19 and Prom1 overexpressing WT cells. PCR-1 (exon 3): forward 5′-GGGATGGTGCCTTGAGTGAA-3′; reverse 5′-TGAAAAGGAGTTCCCGCACA-3′, PCR-2 (exon 2): forward 5′-CCATACCTAGGTCCCCGTCC-3′; reverse 5′-TTTAT GACCCGGCTTCTGGG-3′, PCR-3 (exon 4 and exon 6): forward 5′-CAGAAGGCATATGAATCCAAAA-3′; reverse 5′-ATCACCAA CAGGGAGATTGC-3′, PCR-4 (exon 27 and exon 29 UTR): forward 5′-TCATGTATATGGTATTCACAATCCTG-3′; reverse 5′-AGCACTACCCAGAGACCAATG-3′. All four PCR products were treated by exonuclease 1-recombinant shrimp alkaline phosphatase (SAP, New England Biolabs) at 37°C for 45 minutes and 75°C for 10 minutes followed by sequence analysis. Purified PCR products were loaded on a 2% E-gel agarose gel (Thermo Fisher Scientific) and imaged.

Autophagy Assays

Confocal microscopy and flow cytometry methods were used to quantify LC3 puncta, an index for the induction of autophagy. For confocal microscopy, control and KO cells were grown on Mattek glass bottom dishes, and treated with EBSS, 50 μM CQ, or 20 nM RAP for 3 to 4 hours. Lysosomes were identified by the addition of 1 μM Lysotracker Red DND99 to the medium 30 minutes prior to the end of the treatment. Cultures were fixed with 4% paraformaldehyde, permeabilized in ice-cold methanol, blocked, and incubated with primary antibody against LC3-I/II overnight at 4°C followed by incubation with secondary antibody. Nuclei were identified by incubation with 1 μM TO-PRO3 (Invitrogen). Fluorescence was detected using a Nikon Eclipse TE2000 laser scanning confocal microscope. Images were manually thresholded, and the total number of $LC3^+$ and $LC3^+$ lysosomal puncta were automatically counted using NIS elements software (Nikon). We then normalized the total number of puncta per image to the total number of cells in each image. Diffuse LC3 staining was not quantified.

For flow cytometry, control and Prom1-KO cells were treated as described above, rinsed with PBS, and trypsinized. Cells were collected by centrifugation, fixed in ice-cold methanol for 20 to 30 minutes at −20°C or 2% paraformaldehyde for 15 minutes at 25°C, and permeabilized in PERM buffer (BD Biosciences, San Jose, CA, USA) for 30 minutes on ice

followed by blocking with FcγR (BioLegend, San Diego, CA, USA) for 10 minutes. Cells were incubated with Prom1 (1:100), LC3-I/II (1:100) or 0.5 μg LAMP2 (Abcam, Cambridge, MA, USA) antibodies for 1 hour at room temperature, washed, and incubated with Alexa Fluor 488 and Alexa Fluor 647 secondary antibodies (Thermo Fisher Scientific) for 45 minutes. Samples were washed and analyzed with the FlowSight Imaging Flow Cytometer (EMD Biosciences/Millipore Corp.), which simultaneously produced dark field (side scatter), bright field (BF), and fluorescence images at ~20× magnification. Compensation controls were obtained from single color stained cells. The IDEAS software (Amnis Technology, EMD Millipore, Billerica, MA, USA) was used to separate single cells and cell doublets positive for $CD133^+/LC3^+$ or $LC3^+/LAMP2^+$ cells. We used the Spot Counting Wizard in IDEAS to automatically quantify LC3 puncta formation. In order for the Wizard to correctly identify LC3 puncta staining, we manually identified cells expressing low (diffuse) and high (punctate LC3) numbers of LC3 puncta. The wizard used these populations to generate a spot mask, which was applied to count individual spots across our sample population (5000–10,000 cells). A spot count of 3 or greater was considered punctate. Cells with variable levels of LC3 intensity were chosen for the reference population to avoid bias based on LC3 intensity.

LC3-I and LC3-II protein levels were further analyzed by western blotting. To quantify autophagy in RPE cells, we compared (1) the levels of LC3-II to LC3-I and (2) levels of LC3-II to actin. Both quantification methods demonstrated similar conclusions throughout our studies involving primary RPE and ARPE-19 cells.

Relative Hypoxia

Primary RPE cells seeded in six-well clusters were cultured at 20% O_2 and 5% CO_2. After reaching 60% to 70% confluency, the culture medium was changed and treated as 0 hours. For the relative hypoxia experiments, cells were subsequently incubated at 37°C in a controlled environment of 5% CO_2, 8% O_2, and 87% N_2 for the specified time periods. Cells cultured under hypoxic conditions were immediately processed and stored at –80°C.

STR Analysis

The batch of the ARPE-19 cells used in this study was validated by short tandem repeat (STR) analysis performed by the ATCC Cell line authentication service. Briefly, 17 STR loci plus the gender-determining locus, Amelogenin, were amplified using the commercially available PowerPlex 18D kit from Promega, and the cell line sample was processed using the ABI Prism 3500xl Genetic Analyzer. Data were analyzed using GeneMapper ID-X v1.2 software (Applied Biosystems). Our cells were found to be a perfect match for the ATCC human RPE cell line CRL-2302 (ARPE-19). The STR analysis result is a Supplementary File.

Primary RPE and HREC Cultures

Primary human RPE cells were isolated from postmortem deidentified donor eyes provided by the Mid South Eye Bank. The Institutional Review Board at the University of Tennessee Health Science Center approved the use of human eyes from deidentified donors. We used primary RPE cells that were derived from two young donors (age 29 or 40) and from two aged donors (>70 years of age) as described previously.[32] All donor eyes were shipped to our laboratory within 24 hours of enucleation. Globes were excised, anterior segment was removed, vitreous was extracted manually, and the retina was dissected free. The eyecup was washed three times with Dulbecco's modified Eagle's medium (DMEM), and 0.25% trypsin/EDTA was applied for four 15-minute digestion cycles. Cells were loosened by aspiration, transferred to DMEM with FBS, spun at 2000*g* for 5 minutes, and the cell pellet was resuspended in DMEM in 15% FBS and plated in poly-L-Lysine coated 12-well cell culture ware. The fastest growing cells with cobblestone morphology were used for our studies. Primary cultures within the first three to five passages were used for our studies. Stock cells were maintained in DMEM and Ham's F12 medium (1:1) ratio containing L-glutamine and 10% FBS in a humidified, 37°C incubator in an atmosphere of 5% CO_2. RPE cells were cultured using protocols described previously.[33] Briefly, RPE cells were seeded on plastic cell wares and confluent monolayers were used for experiments. For differentiating cultures, RPE cells were seeded on transwell inserts, and the cells were grown for more than 4 weeks in DMEM containing 1% FBS.

The HRECs were cultured in cell-ware pretreated with attachment factor in DMEM:F12 (1:1) media containing 1% penicillin-streptomycin, endothelial cell growth supplement (ECGS; Sigma-Aldrich Corp.) and 10% FBS and grown in 5% CO_2 at 37°C. Medium was changed every 2 days, and cells between three and five passages were used for all experiments.

Western Blotting

Cell lysates were prepared using mammalian protein extraction buffer (Pierce, Rockford, IL, USA) with 150 mM NaCl, 1 mM Na_2 EDTA and a protease inhibitor cocktail followed by SDS-PAGE. Proteins were transferred to Immobilon-P membranes (Millipore, Bedford, MA, USA) and probed with primary antibodies overnight at 4°C in Tris-buffered saline (TBS) containing 0.1% Tween-20 and 5% nonfat dry milk (Bio-rad, Hercules, CA, USA). Membranes were subsequently incubated with horseradish peroxidase-conjugated secondary antibodies at room temperature for 1 hour, and the immunocomplexes were visualized by the ECL detection system (Perkin Elmer, Waltham, MA, USA) using the Kodak Image Station 4000R. Membranes were stripped and reprobed for actin or GAPDH as loading controls. Representative western blots from three experiments are shown. Densitometric analysis of all western blots was performed using Image J software (developed by Wayne Rasband, available at http://rsb.info.nih.gov/ij/index.html, provided in the public domain by the National Institutes of Health).

Immunoprecipitation

RPE cells were rinsed with ice cold PBS and lysed by freeze thawing in NP40 cell lysis buffer (Invitrogen) containing protease and phosphatase inhibitors (Thermo Fisher Scientific). The lysates were transferred to Eppendorf tubes and centrifuged at 12,500 rpm for 15 minutes at 4°C. The cell extracts containing equal amounts of proteins were incubated with the appropriate antibodies overnight at 4°C, followed by the addition of protein A/B Sepharose CL4B beads (GE Healthcare 71-7089-00 AE) with gentle rocking for 2 hours. The beads were washed three times with lysis buffer and once with PBS, and the immunocomplexes were released by heating in Laemmli sample buffer and analyzed by western blotting using specific antibodies.

Statistical Analysis

All data are expressed as mean ± SE. Experiments were repeated three times, with triplicate samples for each. ANOVA and Bonferroni post hoc testing determined the significance of

Investigative Ophthalmology & Visual Science

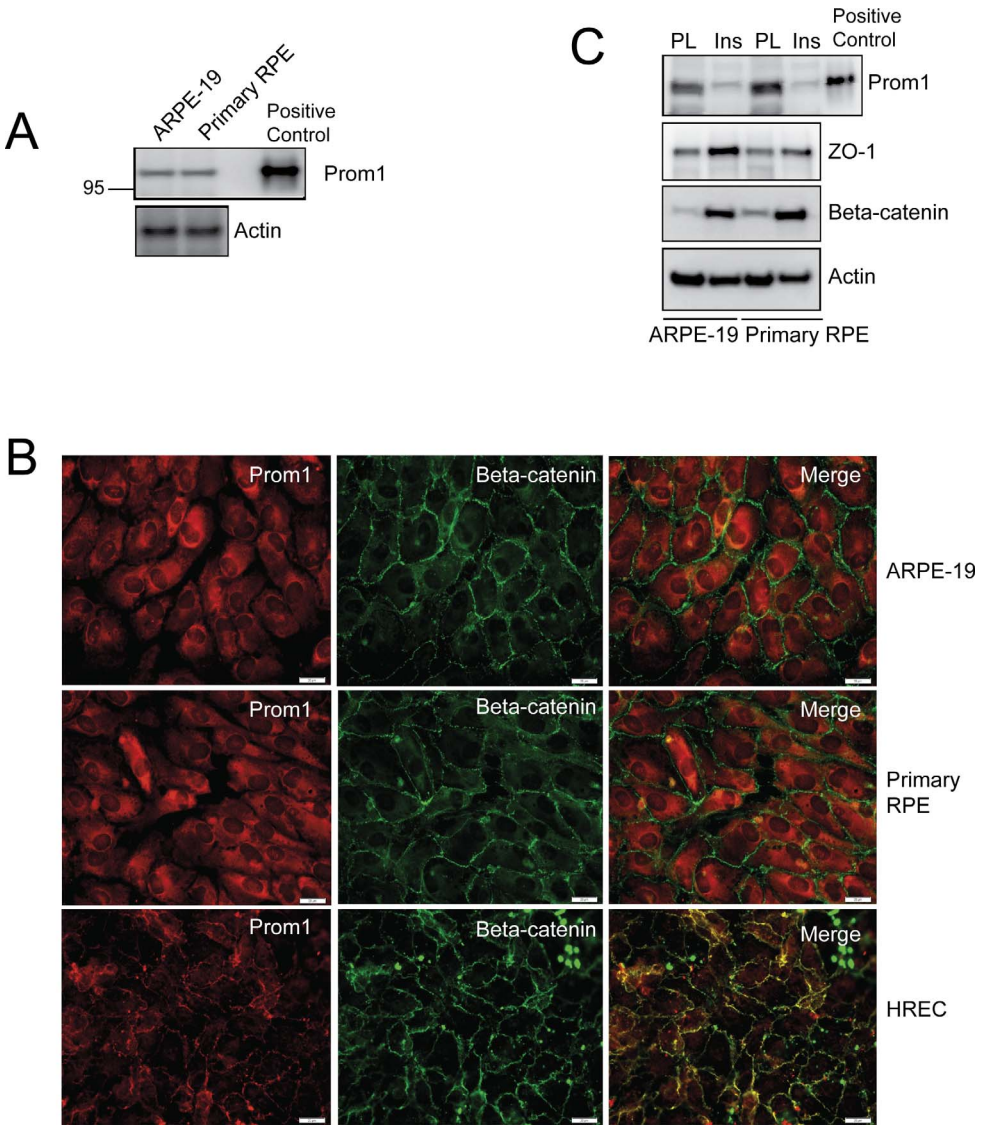

Figure 1. Expression and localization of Prom1 in human RPE. (**A**) ARPE-19 and primary human RPE cells were analyzed for Prom1 expression using an antibody specific for Prom1. (**B**) Data show immunolocalization of Prom1 in ARPE-19, primary RPE cells, and primary HRECs by confocal microscopy. *Scale bar*: 20 μm. (**C**) Representative immunoblots showing ZO-1, Prom1, and β-catenin in both ARPE-19 and primary RPE cells grown on plastic (PL) cell ware and transwell inserts (Ins).

the differences between means. Values of $P < 0.05$ were considered significant.

Results

Expression and Localization of Prom1 in RPE Cells

We investigated the expression and localization of Prom1 in both immortalized ARPE-19 cells and primary RPE cultures obtained from donor eyes. Similar levels of Prom1 expression were observed in ARPE-19 cells and primary RPE cultures (Fig. 1A). Immunofluorescence staining of Prom1 and β-catenin expression show that Prom1 is mainly distributed in the cytoplasm and perinuclear regions with some nuclear staining in the ARPE-19 and RPE cultures, which failed to co-localize with peripheral β-catenin (Fig. 1B). Prom1 does co-localize with β-catenin in HRECs, confirming that the antibody can detect Prom1 in the cell membrane. This suggests that, surprisingly, Prom1 is intracellular and does not localize to the RPE cell membranes at the intercellular junctions.

To further investigate Prom1 expression, we used confluent primary RPE and ARPE-19 monolayers grown on plastic cell culture-ware or differentiated RPE cultures using prolonged growth on transwell inserts as performed previously,[34] and examined Prom1 expression using western blotting. Differentiation of RPE was associated with the increased expression of ZO-1 and β-catenin and decrease in Prom1 expression, compared to nondifferentiated RPE (Fig. 1C), suggesting a correlation between reduced Prom1 expression and RPE differentiation.

Prom1 Regulates Autophagy in RPE Cells

Since Prom1 localized to the cytoplasm in RPE cells (Fig. 1B) and cytoplasmic localization of Prom1 has been correlated with increased autophagy in hepatoma cells,[12] we performed experiments to investigate the role of Prom1 in autophagy in the RPE. Prom1 expression was significantly downregulated in

Investigative Ophthalmology & Visual Science

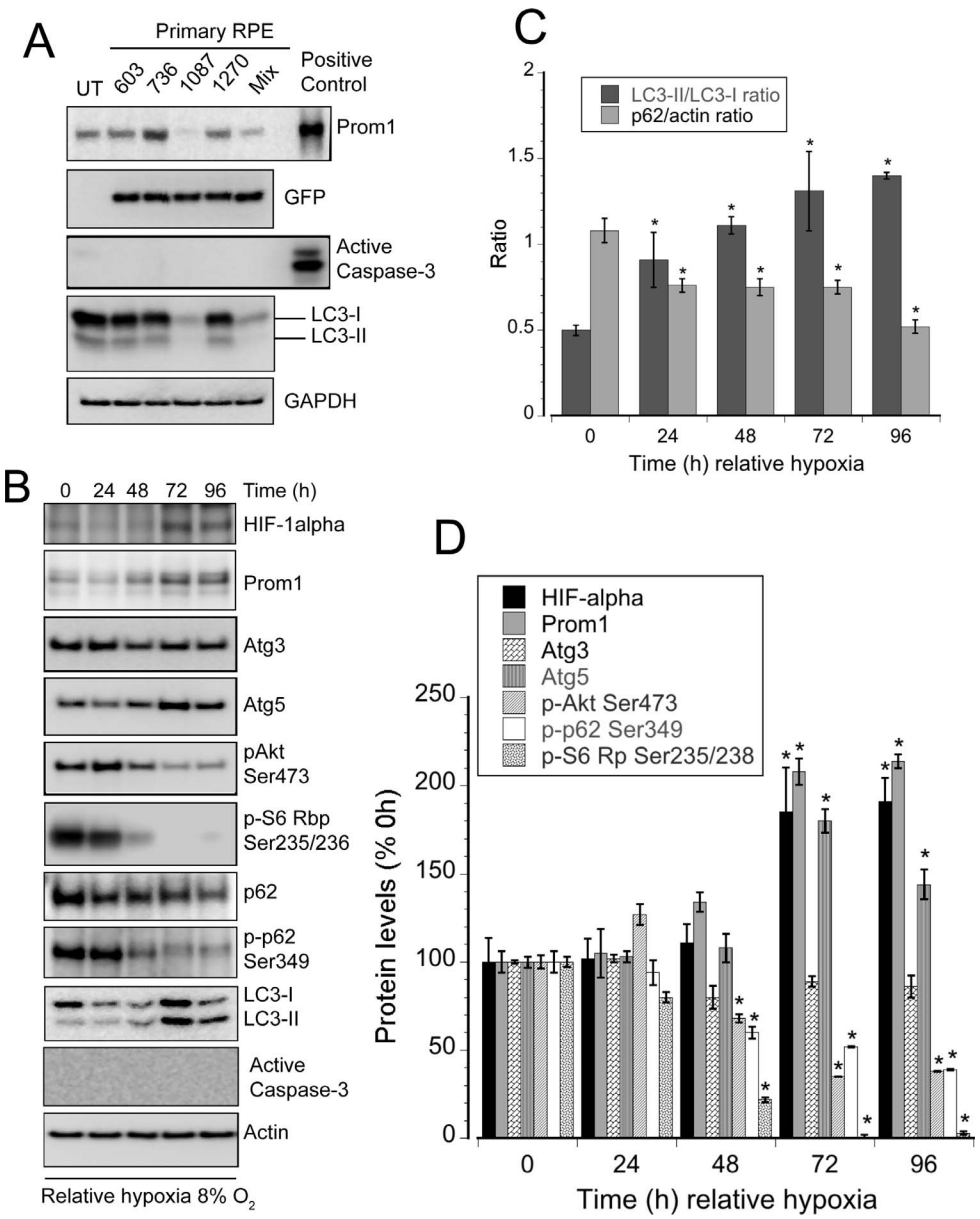

Figure 2. Mild hypoxia induces Prom1 and autophagy in primary RPE cells. (**A**) Data show the levels of Prom1, GFP, LC3-I/LC3-II, and active caspase-3 in primary RPE cells stably transfected with Prom1-siRNA-lentivirus. (**B**) Data show the levels of HIF-α, Prom1, Atg3, p-Akt Ser473, p62, p-p62 Ser349, and LC3-I/LC3-II in primary RPE cultures exposed to hypoxia with 8% oxygen and 5% CO_2 for the indicated time periods. (**C**) LC3-I/LC3-II and p62 densitometric analysis of data shown in **B**. *Significantly different compared to cells at 0 hours ($P < 0.05$). (**D**) Densitometric analysis of results shown in **B**. Values from 0-hour cells were set at 100%. *Significantly different compared to 0-hour cells ($P < 0.05$).

RPE cells stably transfected with Prom1-siRNA (construct 1087, Fig. 2A) and partially blocked when all four siRNA constructs were used. Upon induction of autophagy, microtubule-associated protein light chain-I (LC3-I) is conjugated by Atg7, Atg3, and Atg-5 multimers to the lipophilic phosphatidyl-ethanolamine to generate LC3-phosphatidylethanolamine conjugate (LC3-II), which is recruited to autophagosomal membranes and whose levels correlate with autophagosome number.[35,36] Knockdown of Prom1 with construct 1087 dramatically decreased levels of both LC3-I and LC3-II (Fig. 2A), suggesting that Prom1 is a novel regulator of autophagy in RPE cells. The mixture of all Prom1-siRNA constructs reduced Prom1, LC3-I, and completely reduced LC3-II expression. Since autophagy has been implicated in RPE survival, we hypothesized that inhibition of basal RPE autophagy by Prom1 siRNA might be detrimental for RPE homeostasis, perhaps leading to the induction of caspase-3-dependent apoptosis. Therefore, we measured caspase-3 activation in cells transfected with Prom1 siRNA, and found that caspase-3 was not activated in these cells. These results indicate that inhibition of basal RPE autophagy failed to induce RPE apoptosis (Fig. 2A).

Prom1 Expression Correlates With the Induction of Autophagy in Response to Stressors and Aging in RPE Cells

Extracellular and intracellular stress signals, like hypoxia, oxidative stress, and nutrient deprivation,[37] are known to trigger autophagy. We next examined the role of Prom1 expression on hypoxia- or nutrient deprivation-induced

autophagy signaling. Acute hypoxic exposure (1%–3% oxygen) of RPE cells increases expression of both hypoxic master regulator, HIF-lα, and angiogenic stimulator, VEGF within 12 hours.[38,39] Since reduced oxygen ∼12% is physiologic and is sufficient to induce moderate hypoxia in humans,[40,41] we exposed RPE cells to moderate/relative hypoxia (8% oxygen) for 0 to 96 hours and examined the effect of hypoxia on autophagy and Prom1 expression. HIF-1α expression significantly increased after prolonged hypoxic treatment of 72 hours and remained elevated at 96 hours (Fig. 2B). Autophagy is a dynamic process where LC3-I is rapidly converted to LC3-II. However, the pattern of LC3-I (precursor) to LC3-II (product) conversion is not only cell type specific, but also related to the type of stimulus and the relative levels of LC3-I and LC3-II proteins in various cell types.[42] Primary RPE cells exposed to hypoxia for 24 hours showed a significant reduction of LC3-I without increasing LC3-II levels (Fig. 2B). Both LC3-I and LC3-II levels showed a similar pattern after 48 hours of hypoxia, indicating a rapid interconversion of LC3-I to LC3-II followed by consumption of the LC3-II protein. Both LC3-I and LC3-II protein levels increased after 72 hours of relative hypoxia. However, LC3-I levels decreased and LC3-II expression remained elevated after 96 hours of hypoxia. Although LC3-II levels are commonly normalized to actin to measure autophagy, actin levels may decrease when autophagy is induced in many organisms ranging from yeast to mammals.[42] Furthermore, ignoring the changes in LC3-I in favor of LC3-II normalized with actin[43] may not provide an accurate picture of the autophagic response in RPE cells. Since the ratio of LC3-II to LC3-I was previously used to monitor autophagy flux in the retina,[44] we used LC3-II/LC3-I ratio as an index for autophagy activation in primary RPE cells. Measuring LC3-II to LC3-I ratio showed activation of autophagy in primary RPE cells within 24 hours of moderate hypoxia, which increased throughout the entire time period of hypoxia treatment (Fig. 2C). BAF is a specific inhibitor of vacuolar-type ATPase (V-ATPase) and is known to prevent the fusion of autophagosomes with lysosomes resulting in an inhibition of autophagy.[45] Exposure of primary RPE cells with 48 hours of hypoxia in the presence of BAF further increased LC3-I and LC3-II accumulation, suggesting activation of autophagy flux in response to hypoxia (Supplementary Fig. S1). To confirm whether cells exposed to 96 hours of hypoxia were undergoing apoptosis, samples were analyzed for activation of caspase-3. Data presented demonstrate that moderate hypoxia for 96 hours failed to activate caspase-3, indicating sustained autophagy exerts a protective effect during hypoxia in primary RPE cells. p62 is also commonly used as a marker for the induction of autophagic flux[46] as p62 levels are inversely correlated with the induction of autophagy. Moderate hypoxia reduced p62 expression at 24 hours, which continued to decline in a time-dependent manner (Figs. 2B, 2C). Likewise, phosphorylation of p62 Ser349 decreased in response to hypoxia in a time-dependent manner. Exposure to hypoxia for 72 to 96 hours significantly increased expression of Prom1, Atg5, and LC3-II/LC3-I ratio, without altering Atg3 expression (Figs. 2B–D). Although hypoxia increased autophagy within 24 hours, no significant changes in Prom1 were noted at this time point, indicating that sustained activation of autophagy in response to prolonged moderate hypoxia correlates with increased expression of Prom1. Furthermore, these results also suggest that Prom1 may play a direct or indirect role in the activation of autophagy.

Both mTORC1 and mTORC2 are negative regulators of autophagy, and phosphorylation of ribosomal protein S6 at Ser 235/236 (p-S6 Rp) and phosphorylation of Akt at Ser473 (p-Akt) are surrogate markers of mTORC1 and mTORC2 activation, respectively.[26,47,48] Thus, we examined the activation of p-S6 Rp and Akt in RPE cells exposed to hypoxia. Hypoxia significantly decreased phosphorylation of p-S6 Rp at 48 hours, which was completely abolished at later time points. Furthermore, hypoxia decreased phosphorylation of p-Akt after 48 to 96 hours of hypoxia (Figs. 2B, 2D). These results suggest that both mTORC1 and mTORC2 activities are inhibited by hypoxia.

Amino acid starvation is a potent inducer of autophagy. Amino-acid deprivation of ARPE-19 cells by EBSS rapidly increased levels of LC3-II, Atg5, and Atg7 within 3 hours (Figs. 3A–C). After 6 to 9 hours of EBSS treatment, LC3-I levels decreased but LC3-II levels were higher compared to untreated cells. Both LC3-I and LC3-II levels were significantly reduced after 18 hours of EBSS treatment, due to lack of amino acid in the culture medium and sustained induction of autophagy. Similar to the effects of hypoxia on LC3 levels, LC3-II expression did not progressively increase in ARPE-19 cells treated with EBSS for 6 to 18 hours. Thus, normalization of LC3-II with actin in response to EBSS treatment cannot be used to demonstrate activation of autophagy in ARPE-19 cells. Because, LC3-I levels decreased with time in ARPE-19 cells (Fig. 3A) and intense autophagy flux has been associated with consumption of LC3-II protein,[49] we used LC3-II to LC3-I ratio to monitor changes in autophagy. The ratio of LC3-II to LC3-I showed time-dependent induction of autophagy in nutrient-deprived ARPE-19 cells (Fig. 3B). EBSS treatment increased phosphorylation of p62 Ser349 and its expression at 3 to 6 hours and gradually declined thereafter, indicating sustained activation of autophagy after prolonged amino-acid deprivation (Figs. 3A–C). Similar to the effects of hypoxia, EBSS inhibited Akt activation after 6 hours and decreased p-S6 Rp within 3 hours (Figs. 3A–C), which was completely blocked thereafter, indicating complete inhibition of mTORC1 and mTORC2 activities in response to nutrient deprivation. Importantly, Prom1 expression significantly increased between 3 and 6 hours of nutrient deprivation, which later returned to levels seen in control cells (Figs. 3A, 3C). To confirm the correlation of Prom1 with autophagic activity, we used flow cytometry, which was used successfully for assessing autophagy in cultured cells.[42] ARPE-19 cells treated with EBSS for 3 hours showed significant increase of endogenous Prom1 (CD133) intensity, which correlated with increased intensity of LC3 (Figs. 3D, 3E) by flow cytometry. These data demonstrate that transient upregulation of Prom1 is associated with autophagy execution in response to amino acid deprivation.

Autophagy proteins and autophagy flux show an age-related increase in human and mouse RPE.[50] Since metabolic stress (by nutrient deprivation) and hypoxia increase Prom1 expression and simultaneously induce autophagy in the RPE, we investigated whether age-related induction of autophagy was also correlated with Prom1 expression. RPE cells from aged donors show increased LC3-II/LC3-I ratio, Atg5 expression, reduced p62 expression, and increased formation LC3-II puncta (Figs. 4A–D), demonstrating age-related induction of autophagic activity relative to young RPE. Importantly, aged RPE cells also contain higher levels of Prom1 compared to young RPE. To further investigate whether aging activates autophagy flux, young and aged RPE cells were treated with BAF and CQ. CQ is a lysosomotropic agent that was used to inhibit lysosomal enzymes, which in turn leads to the inhibition of both fusion of autophagosomes with lysosomes and lysosomal degradation.[51] Both BAF and CQ increased LC3-II levels in young RPE cells (Fig. 4E). In aged RPE cells, LC3-II/actin ratio significantly increased in response to BAF and CQ treatment when compared to young RPE cells (Figs. 4E, 4F) demonstrating that aging increases autophagy flux. Together, our results suggest a strong relationship between aging, Prom1 expression, and the induction of autophagy in the RPE.

Investigative Ophthalmology & Visual Science

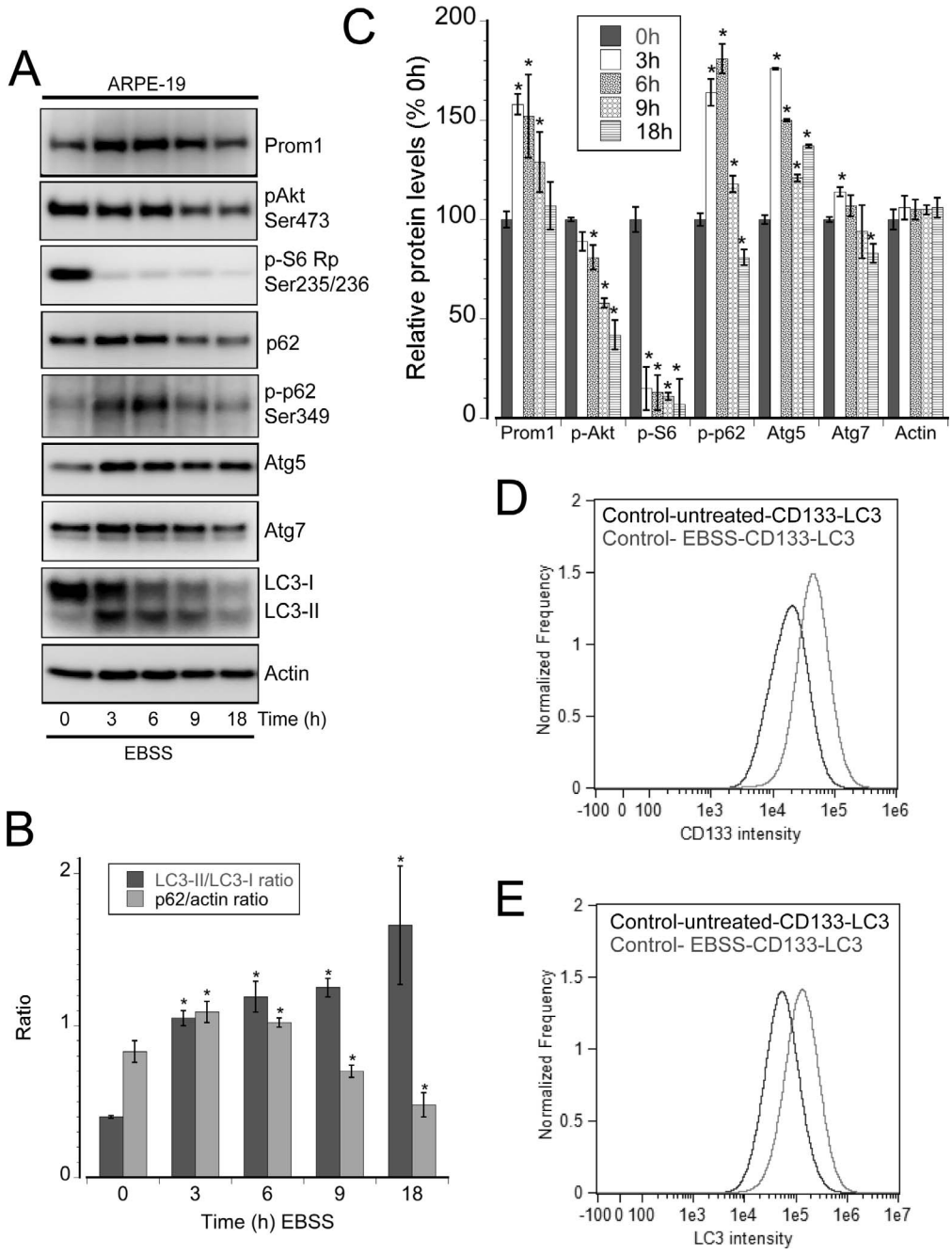

Figure 3. Starvation-induced autophagy correlates with transient upregulation of Prom1 in ARPE-19 cells. (**A**) Data show the levels of Prom1, p-Akt Ser473, p-S6 Ribosomal protein Ser235/Ser236, p62, p-p62 Ser349, Atg5, Atg7, Atg3, and LC3-I/LC3-II in confluent ARPE-19 cells exposed to EBSS for the indicated time periods. (**B**) LC3-I/LC3-II ratio and p62 densitometric analysis of results shown in **A**. *Significantly different compared to 0-hour cells ($P < 0.05$). (**C**) Densitometric analysis of results shown in **A**. Zero-hour values were set at 100%. *Significantly different compared to 0-hour cells ($P < 0.05$). (**D**) Flow cytometry analysis demonstrating CD133 intensity (antibody from Miltenyi) in response to EBSS treatment for 3 hours in ARPE-19 cells. (**E**) Flow cytometry analysis showing LC3 intensity after 3 hours of EBSS treatment in ARPE-19 cells.

Overexpression of WT Prom1 Induces Autophagy via Inhibition of mTORC1 and mTORC2 Activities

Having shown that increased Prom1 expression is correlated with the induction of autophagy, we investigated whether overexpression of Prom1 was able to induce autophagy in the RPE. Since primary RPE cells senesce with cell passage, we used the well-characterized human ARPE-19 cell lines for overexpression of Prom1. We infected ARPE-19 cells with a lentivirus that overexpresses Prom1 (WT) and selected for stably infected cells. WT cells have a robust increase in Prom1 protein (Fig. 5A) and mRNA expression (Fig. 5D), and increased expression of Atg5, Atg7, and the ratio of LC3-II/LC3-I, and decreased pAkt and p-S6 Rp (Figs. 5A–C), indicating that Prom1 is able to activate basal autophagy through upstream inhibition of both mTORC1 and mTORC2. To confirm whether overexpression of Prom1 increases basal autophagy, we used multispectral imaging cytometry that allows multiparametric images of single cells at rates up to 1000 cells/s. Multispectral imaging cytometry was used

Investigative Ophthalmology & Visual Science

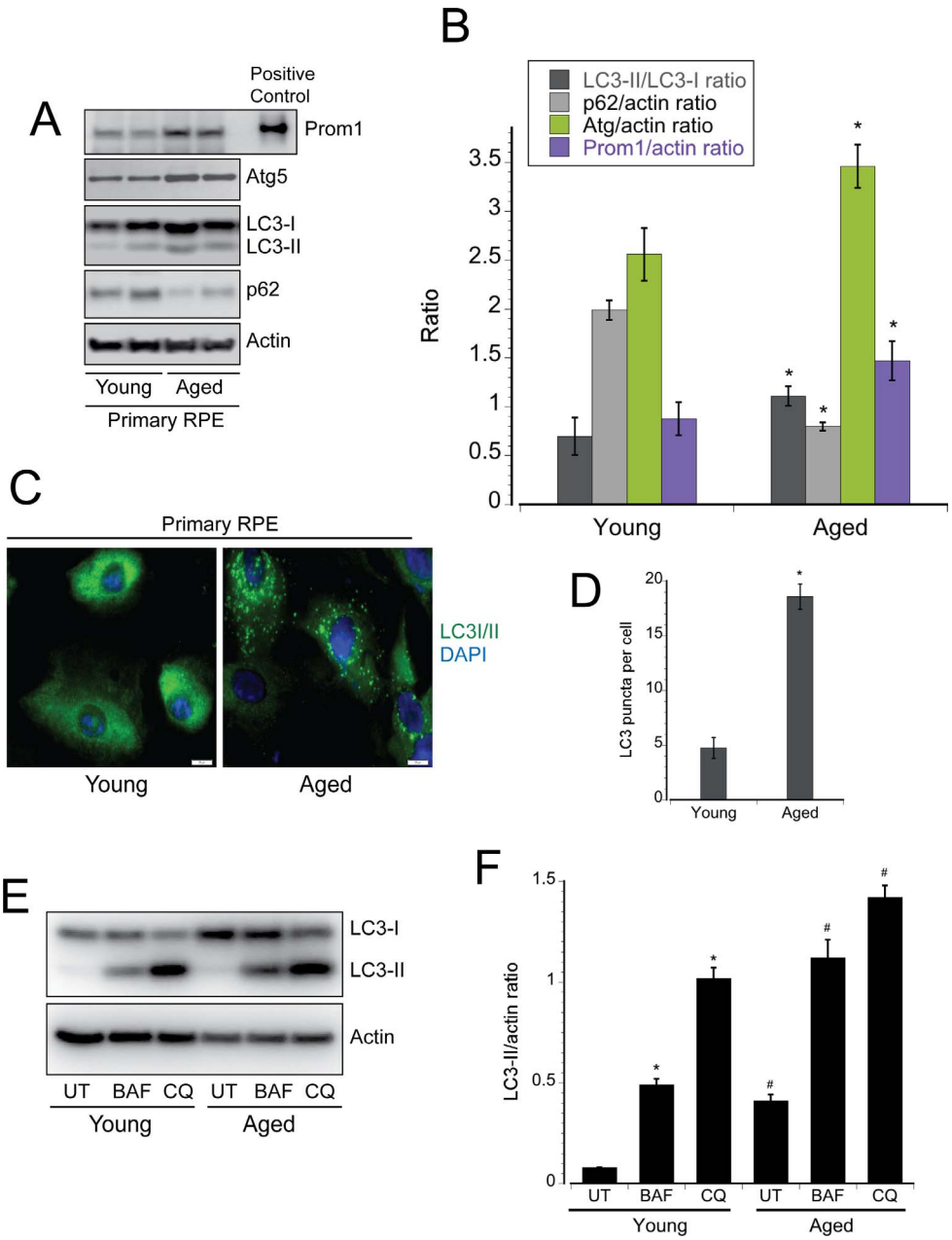

Figure 4. Upregulated Prom1 and autophagy in RPE cells from aged donor eyes. (**A**) Primary RPE cultures from young and aged donors were analyzed by western blot for the expression of Prom1, Atg5, LC3-I, LC3-II, and p62. (**B**) Densitometric analysis of results shown in **A**. *Significantly different compared to young RPE cells ($P < 0.05$). (**C**) Confocal microscopy for LC3 puncta and DAPI in RPE cells obtained from young and aged donors. *Scale bar*, 20 μM. (**D**) Quantification of data presented in **C**. *Significantly different compared to young RPE ($P < 0.05$). (**E**) Young and aged RPE cells obtained from donor eyes were treated with 100 nM BAF or 50 μM CQ for 3 hours and analyzed by western blot for the expression of LC3-I, LC3-II, and actin. (**F**) Densitometric analysis of results presented in **E**. *Significantly different compared to untreated (UT) cells ($P < 0.05$). #Significantly different compared to young RPE cells treated with BAF and CQ, respectively.

previously for assessing autophagy flux in cultured cells.[42] Optimization of image analysis by the IDEAS software and the spot counting wizard (described in the Methods section) allowed us to evaluate Prom1 expression and LC3 spot count in control cells and cells overexpressing Prom1 (Fig. 5E). Our analyses showed that overexpression of Prom1 increased intensity of CD133 (Prom1) green staining (Fig. 5E). Cells overexpressing Prom1 significantly increased basal LC3 spot count >3 in single cells (red staining, Figs. 5E, 5F). To demonstrate changes in autophagic flux, WT cells were treated in the presence and absence of CQ for 3 hours. CQ increased LC3 spot count >3 in control ARPE-19 cells, which further increased significantly in WT cells (Fig. 5G), demonstrating increased autophagic flux.

Although several Prom1 isoforms are expressed in the retina,[52] it is unclear which splice variant is expressed in the RPE. Using RT-PCR, we analyzed expression of Prom1 mRNA transcript variant 3 in the RPE. Since Prom1 retina isoforms differ on the presence or absence of exons,[52] specific primers for the amplification of various exons of transcript variant 3 were used. In control ARPE-19 cells, mRNA was detected from exons-2, 3, 4, 6, and exons 27 and 29 from the UTR region

Investigative Ophthalmology & Visual Science

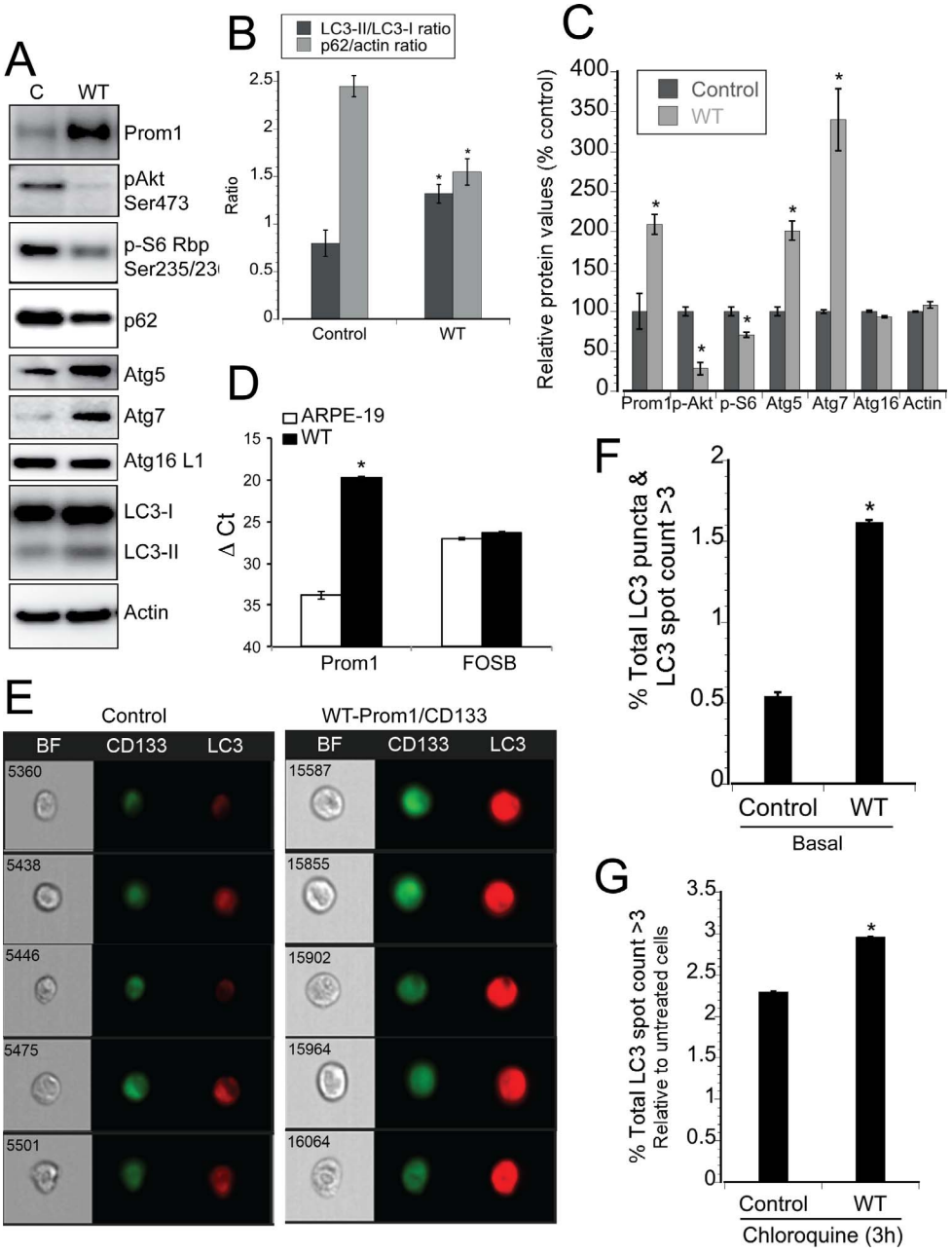

Figure 5. Overexpression of Prom1 downregulates mTORC1 and mTORC2 signaling and upregulates autophagy in ARPE-19 cells. (**A**) Data show the levels Prom1, p-Akt Ser473, p62, Atg5, Atg7, Atg16L1, and LC3-I/LC3-II in ARPE-19 cells infected with purified Prom1-lentivirus (WT) and control ARPE-19 cells. (**B**, **C**) Densitometric analysis of results shown in **A**. *Significantly different compared to control cells ($P < 0.05$). (**D**) mRNA expression from ARPE-19, and WT-Prom1 cultures were analyzed by qRT-PCR for expression of Prom1 and FOSB. Cycle threshold values for each transcript were analyzed using the Δ Ct method. *Significantly different compared to control cells ($P < 0.05$). (**E**) BF, Prom1/CD133, and LC3 images from untreated control and WT single cells using multispectral imaging cytometry. (**F**) The spot counting wizard of the IDEAS software was used to quantify the number of LC3 puncta (that are more than 3) within each cell image. *Significantly different compared to control cells ($P < 0.05$). (**G**) Control and WT cells were treated in the presence and absence of CQ for 3 hours. Data showing LC3 Spot counts greater than 3 relative to cells untreated with CQ. *Significantly different compared to control cells treated with CQ ($P < 0.05$).

(data not shown) of Prom1 variant 3. Since the lentiviral Prom1 construct used to generate the WT cells contained the cDNA sequence ranging from 236 to 2806 bp, mRNAs from all exons of Prom1 transcript variant 3 were detected in these cells except for exons 27 and 29 from the UTR region (PCR-4). This absence is a negative control, showing the UTR region (exon 27 and 29) is after the stop codon in WT cells. Sequence analysis of the purified PCR products (data not shown) confirmed that lentivirus-mediated overexpression of Prom1 (WT) results in the expression of the same transcript variant 3.

In order to confirm the effects of Prom1 on autophagic flux and LC3 processing, both control cells and WT cells were treated with BAF for various time periods. The ratio of LC3-II to LC3-I is regarded as a critical indicator of autophagic activation in RPE cells.[27] In control cells, 100 nM BAF increased LC3-II/LC3-I ratio from 1 to 3 hours, and robustly increased p62 expression from 1 to 3 hours (Figs. 6A, 6B). In WT cells, BAF

Investigative Ophthalmology & Visual Science

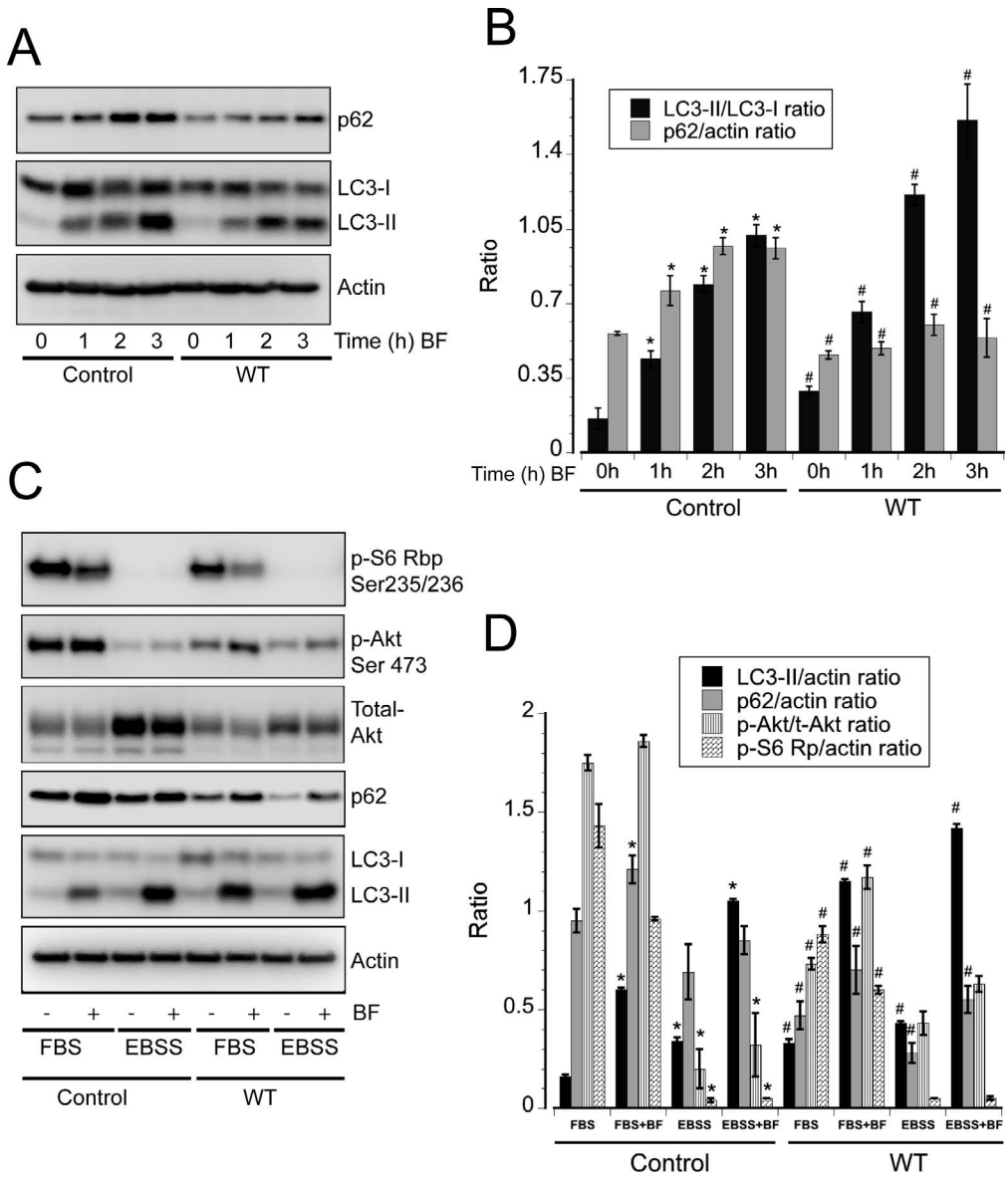

Figure 6. Overexpression of Prom1 increases autophagic flux through inhibition of mTORC1 and mTORC2 in the RPE. (**A**) Representative immunoblots showing LC3-I/II and p62 in control (parental ARPE-19) and Prom1 overexpressing (WT, ARPE-19) cells treated with 100 nM BAF for the indicated time periods. (**B**) Densitometric analysis of results presented in **A**. *Significantly different compared to control cells at 0 hours ($P < 0.05$). #Significantly different compared to control cells in the presence or absence of BAF for the indicated time periods ($P < 0.05$). (**C**) Control and Prom1 overexpressing cells (WT) were treated with or without 100 nM BAF in FBS or EBSS containing medium for 3 hours. Cell lysates were analyzed for p-Akt Ser473, total-Akt, p-S6 Ribosomal protein Ser235/236, p62, LC3-I, and LC3-II. (**D**) Densitometric analysis of results presented in **C**. *Significantly different compared to control cells in the presence of FBS ($P < 0.05$). #Significantly different compared to respective control group ($P < 0.05$).

further increased LC3-II/LC3I ratio in a time-dependent manner (Figs. 6A, 6B). However, the levels of p62 accumulation in response to BAF were significantly lower compared to control cells, suggesting increased autophagic flux and rapid LC3-II consumption in WT cells.

We next verified if autophagic flux was potentiated in response to Prom1 overexpression. Control ARPE-19 and WT cells were cultured in the presence or absence of BAF in normal growth media (FBS) or amino acid starvation media (EBSS). Consistent with data presented in Figure 6A, BAF increased LC3-II accumulation in control cells. EBSS alone decreased LC3-I and partially increased LC3-II, whereas EBSS+BAF decreased LC3-I but robustly increased LC3-II expression in control cells. In Prom1 overexpressing WT cells, BAF alone increased LC3-II, which was higher compared to control ARPE-19 cells. Interestingly, EBSS decreased LC3-I and increased LC3-II levels in WT cells, and BAF further increased LC3-II levels in EBSS treated WT cells. Because LC3-II levels rapidly increased in WT cells, we used LC3-II/actin ratio and p62/actin ratio to measure autophagy in WT cells. WT cells under normal growth conditions have increased LC3-II/actin ratio, and decreased levels of p62/actin ratio, phosphorylation of Akt, and S6 Rp showing constitutive and sustained activation of autophagy. This response was enhanced by BAF treatment (Figs. 6C, 6D). EBSS treatment in WT cells further increased LC3-II/actin ratio and decreased p62, p-Akt, and p-S6 Rp expression, confirming potentiation of autophagy. An enhanced response was observed for WT cells treated with

Investigative Ophthalmology & Visual Science

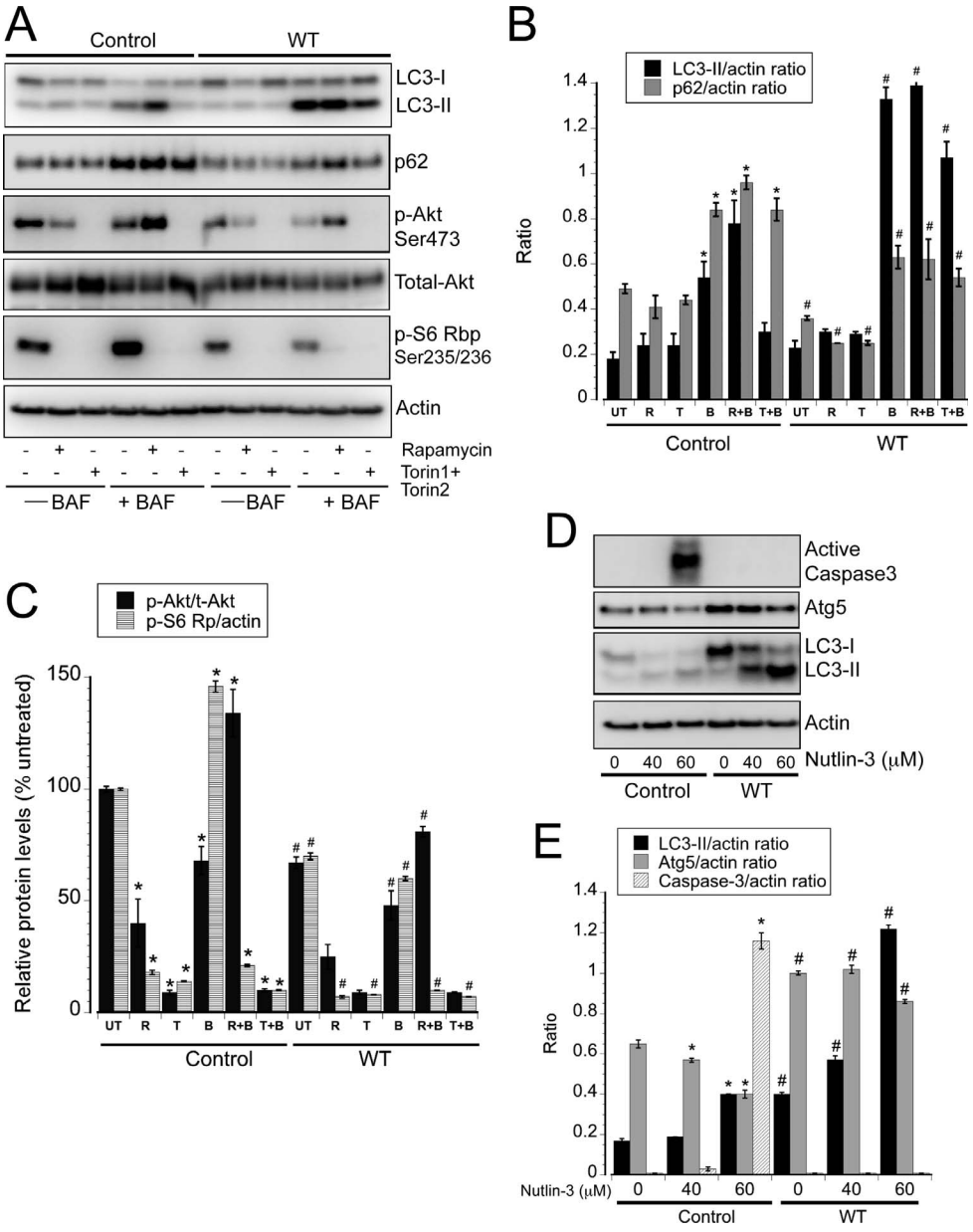

Figure 7. mTOR inhibitors potentiate autophagy flux in cells overexpressing Prom1 and enhancement of autophagy confers protection from Nutlin-3-induced apoptosis. (**A**) Representative immunoblots showing the levels of LC3-I/LC3-II, p-Akt Ser473, total-Akt, p-S6 Ribosomal protein Ser235/236, and p62 in control and Prom1 overexpressing ARPE-19 cells (WT) treated with 1.5 μM RAP or Torins (T; 1.5 μM Torin1 plus 3 μM Torin2) in the presence and absence of 100 nM BAF for 3 hours. (**B**) Densitometric analysis of LC3-II and p62 data presented in **A**. *Significantly different compared to untreated (UT) control cells ($P < 0.05$); #Significantly different compared to corresponding control group ($P < 0.05$). (**C**) Densitometric analysis of results presented in **A**. Values from control untreated (UT) cells were set at 100%. *Significantly different compared to UT cells ($P < 0.05$); #Significantly different compared to corresponding control group ($P < 0.05$). Overexpression of Prom1 induces autophagy but inhibits apoptosis. (**D**) Data showing LC3-II/actin ratio, active caspase-3, and Atg5 levels in control and Prom1 overexpressing cells treated with varying doses of Nutlin-3 for 3 hours. (**E**) Densitometric analysis of results presented in **A**. *Significantly different compared to cells untreated with Nutlin-3 ($P < 0.05$). #Significantly different compared to control cells treated with or without Nutlin-3 ($P < 0.05$).

EBSS+BAF (Figs. 6C, 6D), demonstrating that Prom1 overexpression potentiates autophagy flux in response to BAF and amino acid starvation.

Next, we compared the correlation between mTOR activity and the induction of autophagy in control (parent ARPE-19) and WT cells using three different mTOR inhibitors, RAP, or both Torin1 and Torin 2. RAP is an allosteric inhibitor of mTOR and partly suppresses mTORC1 function, whereas both Torin 1 and Torin 2 are catalytic inhibitors and are capable of completely blocking both mTORC1 and mTORC2 activities.[53,54] Consistent with our previous observations (Fig. 6), BAF increased both p62 and LC3-II/actin ratio mainly due to the impaired fusion of autophagosomes with lysosomes. Compared to control cells at the corresponding treatment, WT cells have decreased p62, and p-S6 Rp expression, indicating activation of autophagy (Figs. 7A–C). This trend was observed for all treatment groups and was further enhanced when cells were co-treated with BAF. Notably, BAF significantly increased LC3-II/actin ratio in WT cells co-treated with RAP and Torins, demonstrating increased autophagic flux.

Since the mTOR inhibitors+BAF potentiated LC3-II/actin ratio in WT cells, we measured Akt and p-S6 phosphorylation. Basal levels of Akt/total Akt ratio were low in WT cells and treatment of WT cells with RAP, Torins, or Torins+BAF failed to significantly decrease p-Akt/total Akt ratio compared to control cells. However, these mTOR inhibitors significantly reduced low basal levels of p-S6 Rp phosphorylation in WT cells in the presence or absence of BAF. Overall, expression of p62 in WT cells treated with mTOR inhibitors in the presence and absence of BAF were considerably lower compared to control cells, indicating increased autophagic flux (Figs. 7A, 7B). Interestingly, BAF treatment in control cells decreased p-Akt/total Akt ratio and increased p-S6 Rp/actin ratio, indicating different roles of BAF on mTORC1 and mTORC2 signaling. This difference was observed for p-S6 Rp to a lesser extent in WT cells treated with BAF alone. Together, these results demonstrate that Prom1 regulates RPE autophagy by negatively regulating both mTORC1 and mTORC2 activities.

To further confirm whether Prom1-dependent RPE autophagy confers cytoprotection, we treated control cells and WT cells with different doses of the nongenotoxic p53 activator, Nutlin-3. Consistent with our previous studies,[32] 40 μM Nutlin-3 had no effect on ARPE-19 apoptosis, but 60 μM Nutlin-3 sensitized cells to apoptosis as evidenced by high levels of caspase-3 activation (Fig. 7D). Concomitant with caspase-3 activation, both 40 μM and 60 μM Nutlin-3 significantly increased LC3-II/LC3-I ratio (Fig. 7E) suggesting that Nutlin-3 is a potent inducer of apoptosis, which in turn induces autophagy in control cells. Nutlin-3 further potentiated autophagy in WT cells in a dose-dependent manner as seen by the higher levels of Atg5 expression and the increase in LC3-II/actin ratio. Importantly, Nutlin-3 failed to activate caspase-3 in cells overexpressing Prom1, indicating that increased autophagic flux confers protection from Nutlin-3-induced apoptosis. The lack of caspase-3 activation in cells overexpressing Prom1 fails to induce proteolytic cleavage of LC3. As a result, the LC3-II/actin ratio in cells overexpressing Prom1 and treated with Nutlin-3 is higher compared to control cells. These results demonstrate that Prom1-dependent induction of autophagy in the RPE does not permit induction of apoptosis in response to nongenotoxic stress.

CRISPR-Mediated Prom1 KO Activates mTOR Signaling and Impairs Autophagy Flux

To further demonstrate the central role of Prom1 in regulation of autophagy, we used Prom1 KO ARPE-19 cell lines (heretofore referred to as KO or KO-6) using the CRISPR-Cas9 lentiviral construct as described in the Methods section. The use of innovative CRISPR technology allows genome editing of the genetic code, typically causing a KO or complete elimination of gene function.[55] We used the 17-nucleotide guide-RNA (gRNA) sequence to target Prom1 gene at exon 10, and selected guides were cloned into the lentiviral backbone. ARPE-19 cells were infected with the purified lentivirus, and genomic analysis of infected cells revealed a Prom1 KO line with one bp insertion and several others with multiple bp deletions. KO and KO-clone 6 were used for our experiments. Both western blotting (Fig. 8A) and real-time PCR (Fig. 8B) confirmed the absence of Prom1 mRNA. KO cells have decreased basal expression of LC3-II/LC3-I ratio, Atg5, and Atg7, and increased p62, p-S6 Rp, and p-Akt expression, compared to control (Cas9) cells (Figs. 8C, 8D), confirming that Prom1 is required for autophagosome maturation, and that Prom1 negatively regulates mTORC1 and mTORC2 signaling. To investigate whether Prom1 regulates autophagosome trafficking to lysosomes, we treated control lentivirus (Cas9) infected and Prom1 KO cells with CQ for 3 hours. Single cells were analyzed by multispectral imaging flow cytometry and IDEAS software for LC3 puncta (Fig. 8E). Our data demonstrate that KO cells had decreased formation of LC3+ puncta and had decreased co-localization of LC3+ with lysosome-associated membrane protein 2 (Lamp2)+ puncta compared to control Cas9 cells (Figs. 8E, 8F).

To further elucidate the involvement of the mTOR/Akt signaling axis in Prom1-mediated autophagy, we treated control Cas9 and KO cells with Torins (using Torin1 and Torin 2) in the presence or absence of BAF. Torins increased Prom1, LC3-II, and decreased p62 expression in control Cas9 cells due to inhibition of mTOR signaling and increased synthesis of autophagosomes. Control cells treated with Torins in the presence of BAF (Torins+BAF) showed higher levels of Prom1, suggesting that autophagy induction in response to mTOR inhibition (by Torins) correlates with increased expression of Prom1 (Figs. 9A, 9B). Higher LC3-II and p62 levels were observed in response to Torins+BAF, indicating that accumulation of LC3-II is due to inhibition of autophagosomal cargo degradation. Torins failed to increase Prom1, LC3-II in KO cells, and lower levels of LC3-II were observed in KO cells treated with Torins+BAF (Figs. 9A, 9B). Unlike WT cells, LC3-I levels remained unaltered in the KO cells after treatment with Torins and Torins+BAF. To compare the LC3 data obtained with WT cells (Figs. 5–7), we used LC3-II/LC3-I to evaluate autophagy in KO cells. Untreated KO cells have decreased LC3-II/LC3-I ratio, and Atg5 expression, and increased p62, p-Akt, and p-S6 Rb expression, suggesting KO cells have increased mTORC1/2 signaling and decreased basal autophagy (Figs. 9A, 9B). Treatment of KO cells with Torins showed significantly lower LC3-II/LC3-I ratio and Atg5, but failed to decrease p62, when compared to control cells. Combined Torins+BAF treatment in KO cells had decreased LC3-II/LC3-I and Atg5 expression, when compared to control cells. Consistent with our previous observations (Fig. 8A), Prom1 KO cells have high basal levels of p-Akt and p-S6 Rp, indicating basal activation of mTORC1 and mTORC2 signaling. However, Torins treatment in KO cells completely inhibited both p-Akt and p-S6 Rp levels (Figs. 9A, 9B) but had no effect on Atg5 expression, showing that inhibition of Akt and S6-Rp is insufficient to induce autophagic activity in the absence of Prom1. Interestingly, KO cells have high levels of p62, which was not altered by either Torins or Torins+BAF treatment, confirming that lack of Prom1 inhibits autophagic flux due to decreased autophagosome maturation and fusion of autophagosomes with lysosomes.

To demonstrate this, we examined LC3 puncta formation in Prom1 KO cells treated with 50 μM CQ (3 hours) or EBSS (3 hours) by confocal microscopy. Since amino-acid starvation by EBSS inhibited mTORC1 and mTORC2 activities leading to the induction of autophagy in ARPE-19 cells (Figs. 3A–C), we used EBSS in control and Prom1 KO cells. Using confocal microscopy, co-localization of LC3 puncta with a lysosomal marker, lysotracker, was used to detect the trafficking of autophagosomes to lysosomes. KO of Prom1 (clone-6) significantly decreased the number of $LC3^{+}$ puncta per cell at baseline and after CQ or EBSS treatment (Figs. 9C, 9D). Co-localization of LC3 aggregates with lysotracker dramatically increased in control cells in response to CQ or EBSS treatment. However, the extent of puncta-lysosome co-localization in response to EBSS was lower compared to CQ-treatment in control cells, showing that CQ specifically inhibits lysosomal degradation, which in turn increases the accumulation of LC3 puncta in lysosomes. The EBSS-induced LC3 puncta was effectively cleared by lysosomal degradation, which prevented its accumulation in control cells. KO of Prom1 (clone-6) significantly decreased co-localization of LC3 puncta with lysosomes after EBSS or CQ treatment (Figs. 9C, 9D). To further validate our observations, we compared LC3 puncta formation

Investigative Ophthalmology & Visual Science

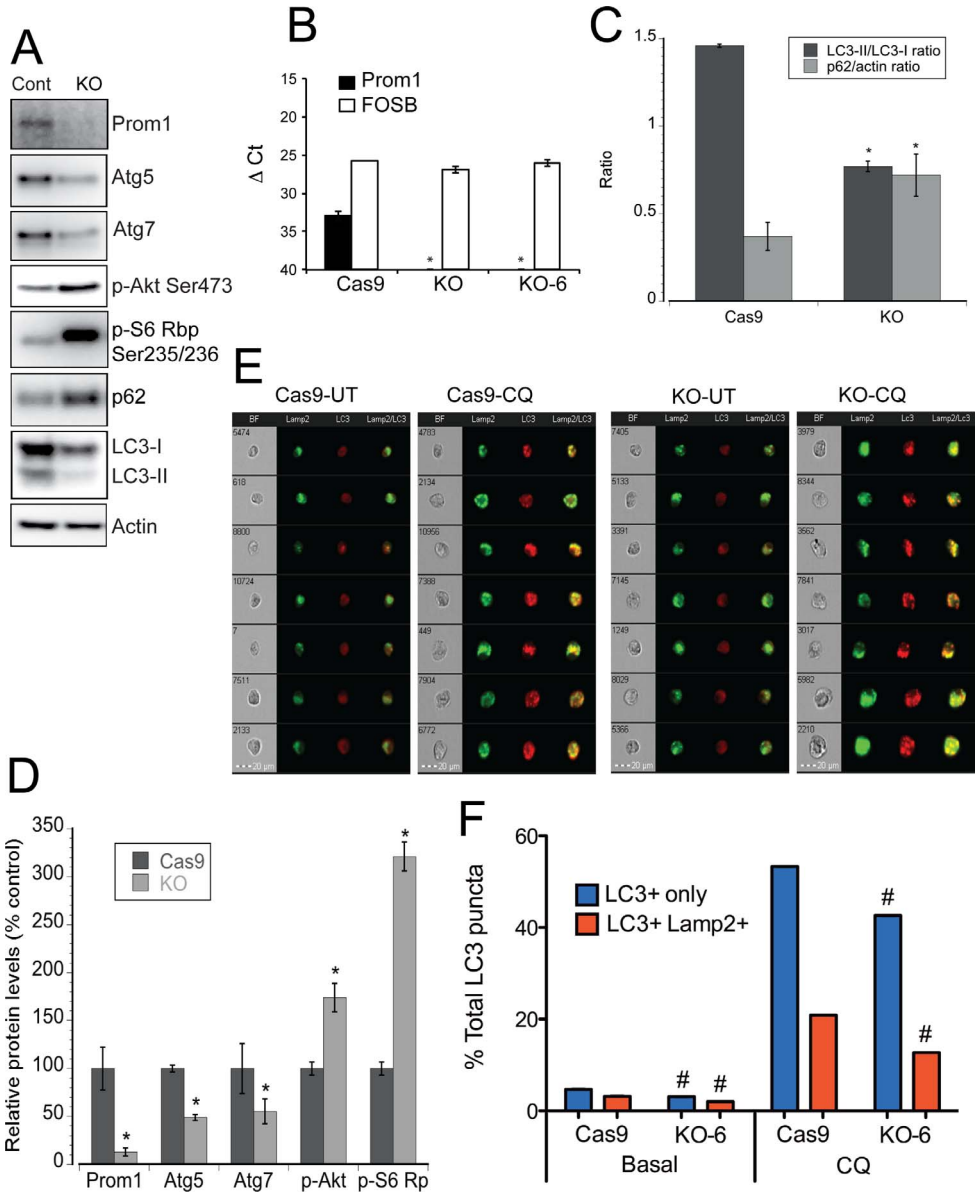

Figure 8. KO of Prom1 decreases basal autophagy through upregulation of mTORC1 and mTORC2 and decreases the number of LC3$^+$ puncta per cell. (**A**) Control and CRISPR-Cas9 mediated Prom1 KO in ARPE-19 cells were analyzed for Prom1 expression. Data show the levels of Atg5, Atg7, p-Akt Ser473, p-S6 Ribosomal protein Ser235/236, p62, and LC3-I/LC3-II. (**B**) mRNA expression from ARPE-19, Cas9-control, Prom1-KO, and Prom1 KO-clone6 cultures were analyzed by qRT-PCR for expression of Prom1 and FOSB. Cycle threshold values for each transcript were analyzed using the Δ Ct method. *Significantly different compared to control cells ($P < 0.05$). (**C**) LC3-II/LC3-I ratio and p62 densitometric analysis presented in **A**. *Significantly different compared to control cells ($P < 0.05$). (**D**) Densitometric analysis of results presented in **A**. Values from control cells were set at 100%. *Significantly different compared to control cells ($P < 0.05$). (**E**) Representative BF, LC3$^+$, Lamp2$^+$ images by FlowSight Imaging Flow Cytometer in Cas9 (control) and KO cells in the presence and absence of CQ. (**F**) %Total LC3$^+$ only or LC3$^+$, Lamp2$^+$ puncta spot count of 3 or greater in Cas9, KO, or KO-6 cells in the presence or absence of CQ. Graph shows ±SE, which ranges from 0.023 to 0.00.3. #Significantly different compared to untreated control cells ($P < 0.001$). Note: There were also significant differences between the Prom1 KO lines at baseline or after CQ treatment ($P < 0.001$).

in control and Prom1 KO cells treated with EBSS (4 hours) or 200 nM RAP (4 hours) by confocal microscopy. Both RAP and EBSS induce autophagy through mTOR inhibition in ARPE-19 cells. These activators of autophagy increased LC3 puncta per cell and their co-localization to lysosomes in control Cas9 cells, which was significantly blocked in KO cells (Supplementary Fig. S2), further confirming that Prom1 is required for biogenesis of autophagosomes and delivery of the autophagosomal cargo to lysosomes in the RPE.

To further elucidate whether stress-dependent induction of autophagy requires the participation of Prom1, we treated control and KO cells with EBSS medium for the indicated time periods (Fig. 10A). Consistent with our previous observations (Fig. 3A), amino-acid deprivation by EBSS significantly increased Prom1 expression at 3 hours in Cas9-infected control cells. Furthermore, EBSS rapidly induced autophagy within 3 hours and sustained activation of autophagy was evident by time-dependent decrease of LC3-I and increase of LC3-II/LC3-I ratio in control cells (Figs. 10A, 10B). Both LC3-I and LC3-II levels were dramatically reduced by 18 hours indicating consumption of LC3 proteins due to sustained activation of autophagy. KO of Prom1 impaired EBSS-induced autophagy,

Investigative Ophthalmology & Visual Science

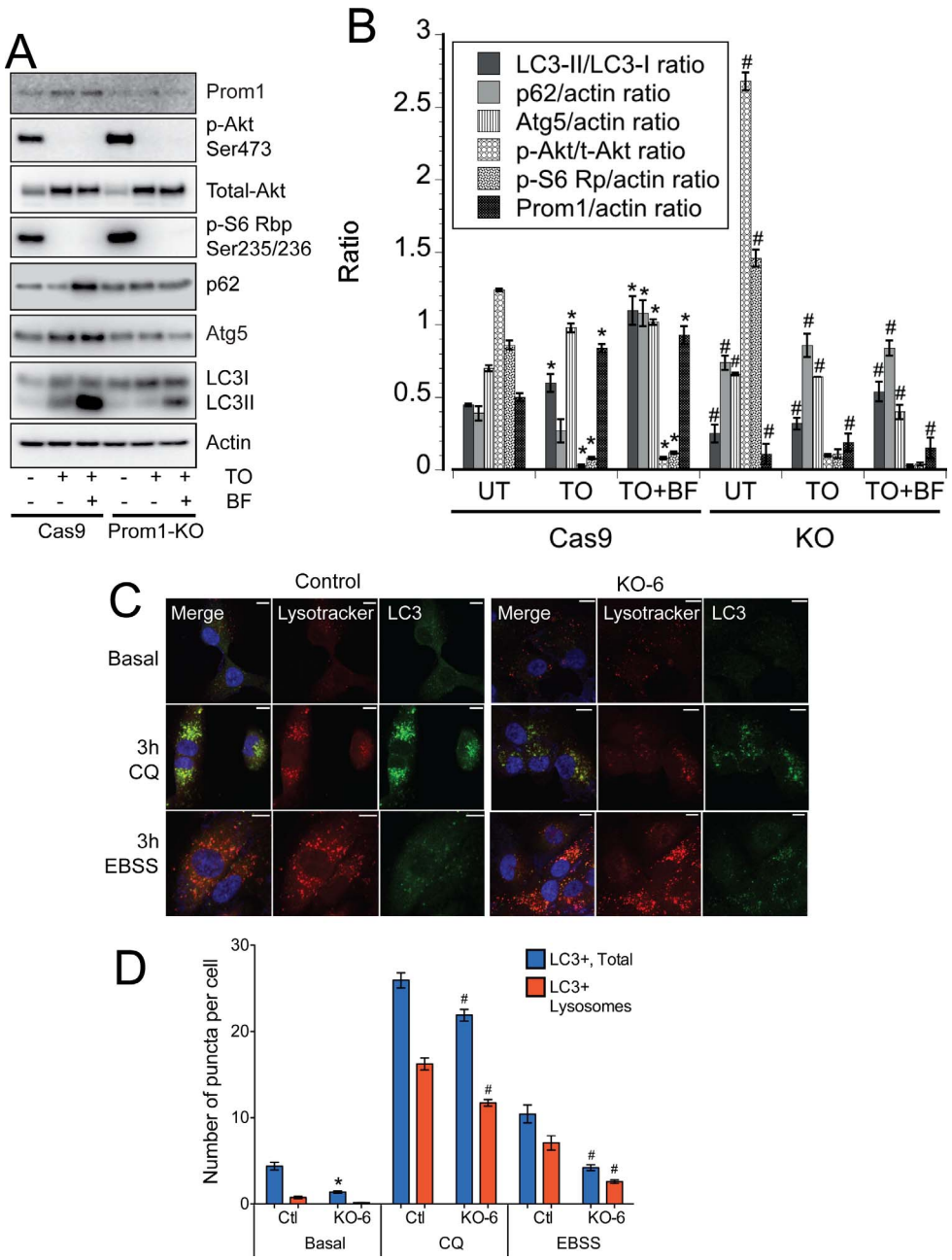

Figure 9. mTOR inhibition fails to induce autophagy in Prom1 KO cells. (**A**) Representative immunoblots of Prom1, p-Akt Ser473, total-Akt, p-S6 Ribosomal protein Ser235/236, p62, Atg5, and LC3-I/LC3-II protein levels in Cas9-control and Prom1-KO ARPE-19 cells untreated or treated with Torins (TO) ± BAF for 3 hours. (**B**) Densitometric analysis of data presented in **A**. *Significantly different compared to untreated (UT) cells ($P < 0.05$). #Significantly different compared to the corresponding control group ($P < 0.05$). (**C**) Representative confocal images showing LC3 (*green*), Lysotracker (*red*), and Merge (*yellow*) in Cas9-control and Prom-KO-clone-6 (KO-6) cells treated with EBSS or CQ for 3 hours. (**D**) Puncta quantification of data presented in **C** using NIS elements software (Nikon). *Significantly different compared to control cells ($P < 0.01$). #Significantly different compared to corresponding controls ($P < 0.001$).

which was evident by unaltered levels of both LC3-I and LC3-II at 3 hours, lower LC3-II levels at 18 hours, and lower LC3-II/LC3-I ratio from 0 to 18 hours compared with control-Cas9 cells. Prom1 KO decreased basal expression of Atg5 and Atg7, and EBSS failed to alter expression of these autophagy-related proteins suggesting that loss of Prom1 decreases autophagic activity. KO cells at 0 hours had high basal levels of p-Akt and p-S6 Rb, which were inhibited or abolished, respectively, in response to EBSS treatment. Although EBSS inhibited these key markers of mTOR signaling in KO cells, it failed to restore autophagy. This indicates that Prom1 deletion constitutively activates mTORC1 and mTORC2 and that inhibition of mTORC1 and mTORC2 activities is insufficient to trigger autophagy in the absence of Prom1. Furthermore, p62 levels remained elevated throughout the entire time period of EBSS treatment strongly (Figs. 10A, 10B) reinforcing the observation that absence of Prom1 impairs normal trafficking of autophagosomes with lysosomes.

Multispectral flow cytometry was also used to demonstrate a role of Prom1 in the biogenesis of autophagosomes in response to amino-acid starvation. Control and KO cells were treated with EBSS for 3 hours and stained with Prom1/CD133

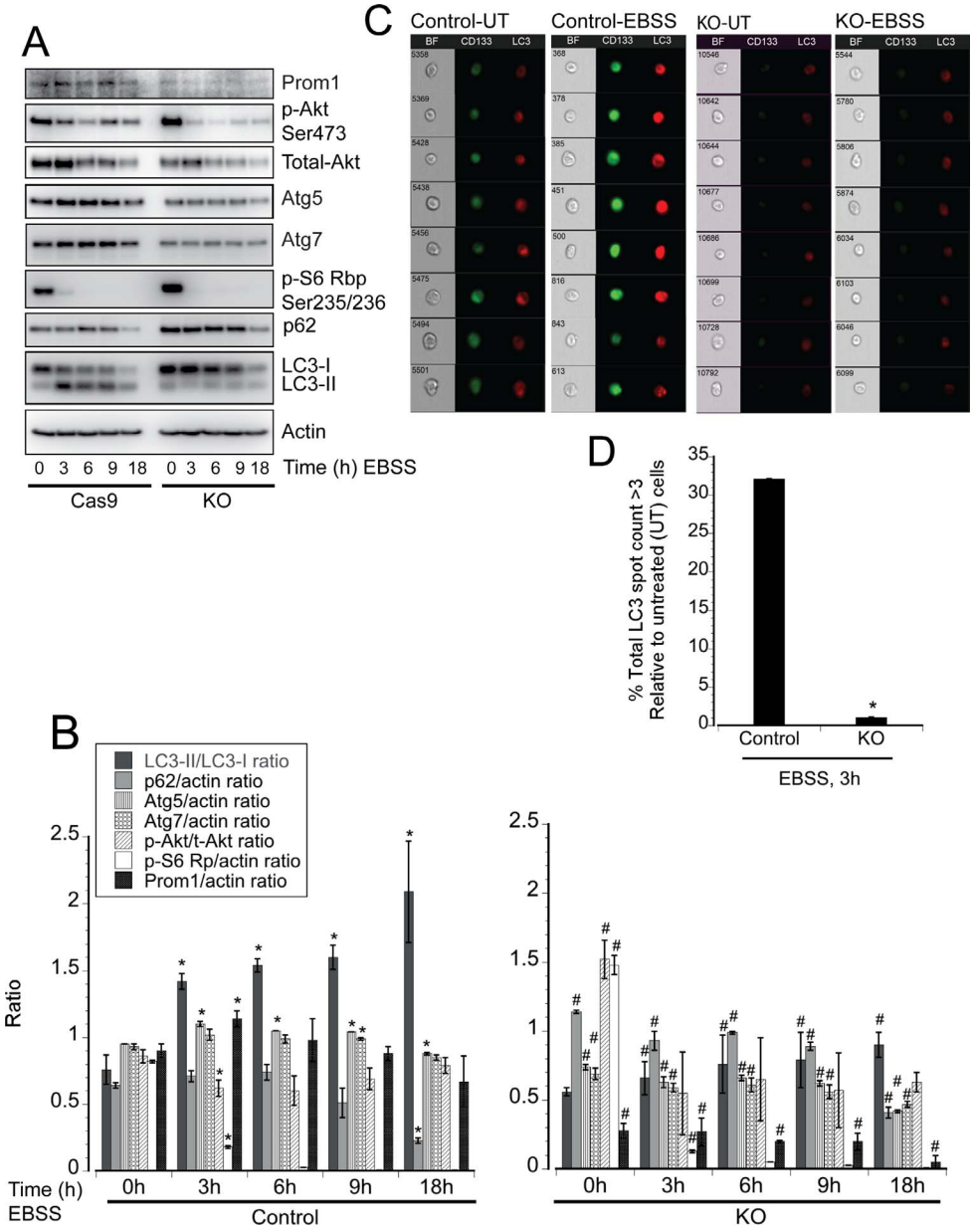

Figure 10. KO of Prom1 impairs starvation-induced autophagy. (**A**) Representative immunoblots showing the levels of Prom1, p-Akt Ser473, Atg5, Atg7, p-S6 Ribosomal protein Ser235/236, p62, and LC3-I/LC3-II in Cas9 and Prom1-KO ARPE-19 cells treated with EBSS for the indicated time periods. (**B**) Densitometric analysis of data presented in **A**. *Significantly different compared to control cells at 0 hours ($P < 0.05$). #Significantly different compared to respective control cells ($P < 0.05$). (**C**) Representative BF, CD133$^+$, LC3$^+$ images by FlowSight Imaging Flow Cytometer in control and Prom1-KO cells in the presence and absence of EBSS for 3 hours. (**D**) % Total LC3 spot count of 3 or greater in control and KO cells in the presence of EBSS relative to untreated (UT) cells. *Significantly different compared to control cells treated with EBSS ($P < 0.05$).

and LC3-I/II specific antibodies. Double positive cells, single positive CD133$^+$ cells, LC3-I/II$^+$ cells, and BF images were analyzed by flow cytometry (Fig. 10C). EBSS robustly increased the number of LC3$^+$ puncta (>3) relative to untreated control cells, but failed to significantly increase LC3$^+$ puncta in Prom1 KO cells (Fig. 10D), again demonstrating that Prom1 is an essential mediator of amino acid starvation-induced autophagy in the RPE.

Prom1 Associates With p62 and Is Required for Autophagosome-Lysosome Fusion

Considering our finding that KO of Prom1 constitutively activates mTORC1 and mTORC2, and inhibition of mTORC1/2 fails to restore autophagic flux in these cells, we hypothesized a significant association between Prom1 and other protein components of the autophagy machinery. To examine this possibility, we immunoprecipitated Prom1 from control ARPE-19 cells and WT cells. p62 was detected in the Prom1 immune complexes from control (both C and empty vector EV infected) cells and at significantly higher levels in WT cells, suggesting that Prom1 interacts with p62, and ectopic overexpression of Prom1 enhances the presence of p62 in the Prom1 immunoprecipitates (Figs. 11A, 11D). Reciprocal coimmunoprecipitation assays showed that p62 was bound to Prom1 in control cells, and WT cells have lower levels of Prom1 bound to p62 (Figs. 11B, 11D), mainly due to decreased p62 levels in WT cells. Prom1, p62, and HDAC6

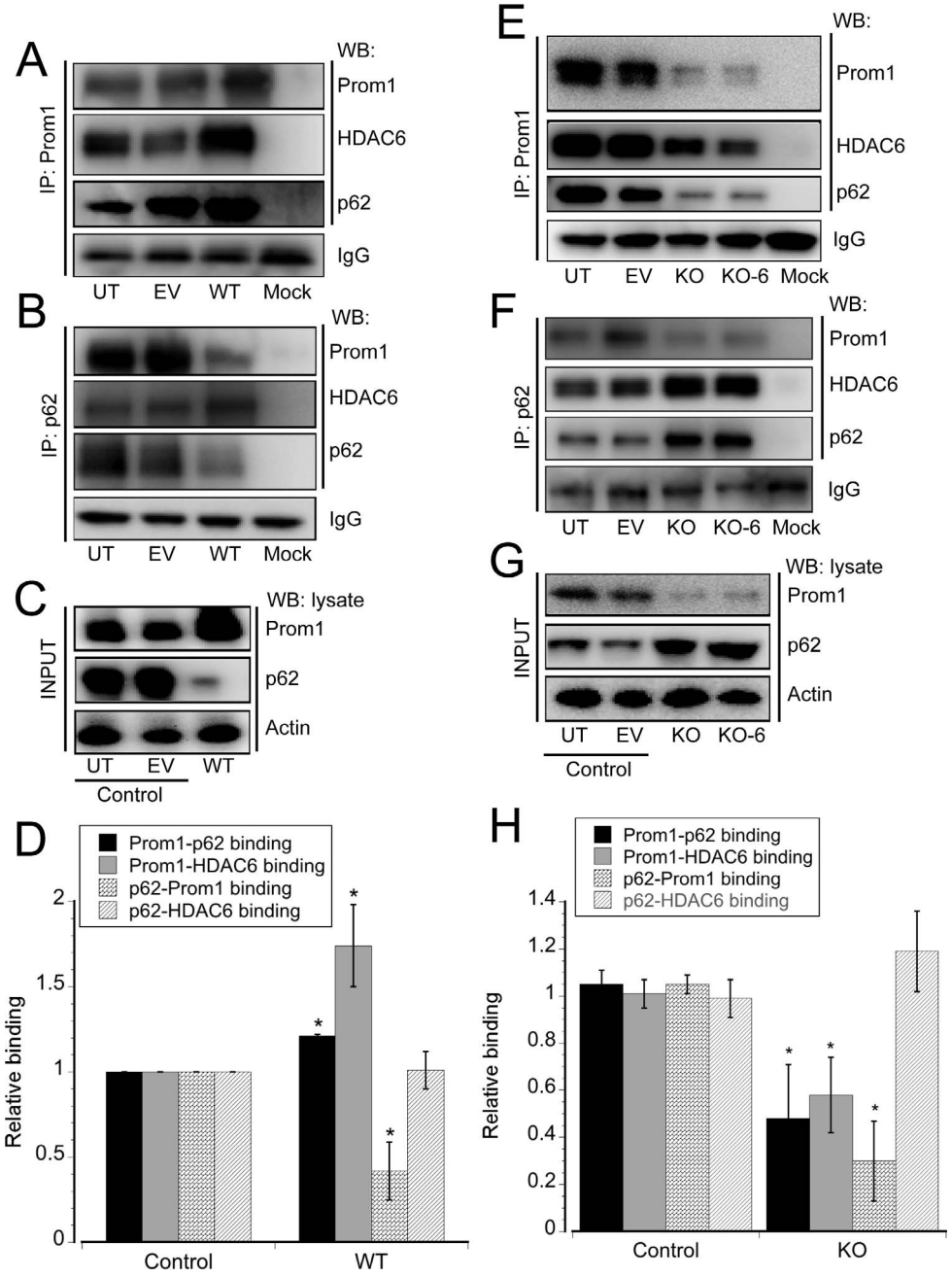

Figure 11. Coimmunoprecipitation of Prom1, p62, and HDAC6. (**A**) Prom1 immunoprecipitates from untreated ARPE-19 control (UT), Cas9 empty lentivirus (EV), and Prom1 overexpressing (WT) cell lysates were analyzed for the presence of Prom1, p62, and HDAC6. The mixture of beads with the respective antibodies was used for mock immunoprecipitation. (**B**) p62 immunoprecipitates were analyzed for the levels of Prom1, HDAC6, and p62. (**C**) Equal amounts of whole cell lysates were simultaneously analyzed for the levels of Prom1, p62, and actin as input. (**D**) Quantification of proteins in Prom1 and p62 immunoprecipitates by densitometry. Control values were set at 100%. *Significantly different compared to untreated control cells ($P < 0.05$). (**E**) Prom1 immunoprecipitates from UT, EV, and Prom1-KO, and KO-6 cell lines were analyzed for the presence of Prom1, HDAC6, and p62. (**F**) Data showing the levels of Prom1, HDAC6, and p62 in p62 immunoprecipitates from control, EV, and KO samples. (**G**) Equal amounts of UT, EV, KO, and KO-6 cell lysates were simultaneously analyzed for the levels of Prom1, p62, and actin as input. (**H**) Densitometric analysis of immunoprecipitation data presented in **D** and **E**. *Significantly different compared to control cells ($P < 0.05$).

bands were undetected in the mock immunoprecipitated samples. Input confirmed increased Prom1 and decreased p62 expression in WT cell extracts (Fig. 11C).

The ubiquitin-binding cytosolic deacetylase-6 (HDAC6) controls autophagy by regulating the fusion of autophagosome with lysosomes. Recent studies show that Prom1 interacts with cytosolic HDAC6,[13] suggesting the possibility that a macromolecular complex comprising of p62, HDAC6, and Prom1 may play a central role in autophagosome maturation and its fusion to the lysosomes. To test the formation of this macromolecular complex, we analyzed Prom1 immunoprecipitates for HDAC6. Endogenous Prom1 was found to associate with HDAC6, and overexpression of Prom1 (WT) increased the amount of HDAC6 in the Prom1 immunoprecipitates (Figs. 11A, 11D). Reciprocal immunoprecipitation with p62 showed the presence of HDAC6 in control cells, but overexpression of Prom1

did not significantly increase the levels of HDAC6 in the p62 immunoprecipitates (Figs. 11B, 11D), showing that Prom1 is not required for p62-HDAC6 association.

In order to further confirm that Prom1 interacts with p62 and HDAC6, we probed control-Cas9 and Prom1-KO cell lines. Immunoprecipitation of Prom1 from control (C and EV) cells contained both Prom1 and p62. Prom1 was not visible in Prom1 immunoprecipitates from KO and KO-6 cells, and the levels of p62 were significantly lower in these immune complexes (Figs. 11E, 11H), showing that absence of Prom1 alters the association of p62 with Prom1. Consistent with previous observations (Figs. 8–10), KO of Prom1 significantly increased p62 expression (input, Fig. 11G). However, reciprocal p62 immunoprecipitates from KO cells contained undetectable levels of Prom1, but higher levels of p62 (Fig. 11F). Prom1 and p62 immunoprecipitates from cells both overexpressing and lacking Prom1 contained comparable levels of HDAC6, indicating that the status of cellular Prom1 does not impact the association of p62 with HDAC6 (Figs. 11D, 11H). Our overall findings suggest that Prom1 is an important component of a macromolecular complex consisting of p62 and HDAC6. Disruption of the Prom1 association with this complex negatively impacts autophagosome maturation and delivery of autophagosomes to lysosomes.

Discussion

The key finding of these studies is that Prom1 is a pivotal regulator of autophagy in the RPE. Our data demonstrate for the first time that overexpression of Prom1 constitutively activates autophagy in the RPE via inhibition of mTORC1 and mTORC2. Conversely, KO of Prom1 impairs RPE autophagy via upregulation of mTORC1/2 activities, suggesting that Prom1 is central to the regulation of autophagy. Our data suggest that this effect is controlled in part due to Prom1's ability to form a macromolecular complex comprising of autophagy proteins p62 and cytosolic HDAC6, and disruption of this interaction by genetic deletion of Prom1 impairs autophagosome biogenesis and causes defects in trafficking of the autophagosomes to the lysosomes. These findings have important implications for the maintenance of RPE homeostasis because defective autophagosomal-lysosomal-phagocytic pathways can lead to ineffective clearance of shed photoreceptor outer segments and cause accumulation of damaged organelles and protein aggregates including lipofuscin-like debris in lysosomes, all of which have been linked with the pathogenesis of age-related retinal diseases, including AMD.

The connection between autophagy and aging is complex and cell-type specific. For instance, aging alone has been implicated in both promoting[27] and inhibiting autophagy in various cell types. Age-related deterioration of vision has been linked to the decline in noncanonical autophagy coupled with a loss of phagocytic activity in the RPE, suggesting that the functional interplay between autophagy and phagocytosis is fundamental to vision.[20] In keeping with this notion, our data show that aging increased classical autophagy in the RPE, supported by increased expression of Atg5, loss of p62 expression, increased levels of autophagic puncta, and increased autophagic flux. Of note, age-related induction of autophagy in the RPE was associated with increased expression of Prom1. Therefore, the induction of Prom1-dependent autophagy during aging may be an intrinsic defense mechanism, which enables the RPE to cope with increased oxidative burden, accumulation of ubiquitinated/nonubiquitinated protein aggregates, and phagocytic activity. Although Prom1 was initially described as a surface antigen in normal hematopoietic stem cells[3] and cancer stem cells,[56] recent studies have demonstrated the presence of Prom1 in normal adult tissues including the retina suggesting that Prom1 has diverse physiological functions beyond the known association with cancer stem cells. Several Prom1 isoforms are expressed in the retina,[52] but there is no Prominin-2 (Prom-2) expression in the eye,[57] which perhaps explains why a Prom1 mutation in the human gene causes retinal degeneration without causing other pathological abnormalities. Prom1's important structural role in the photoreceptor outer segment membrane suggested a similar structural role of the protein in the RPE apical microvilli. Anti-CD133 antibody staining of tissue sections showed expression patterns of Prom1 in the apical surface of the RPE layer,[58] the interface between the neural and epithelial retina, and at the basal part of the outer segment of rods and cones,[8] in the adult mouse. Surprisingly, our studies with human cells in vitro demonstrated that Prom1 is expressed in the RPE, but the protein is primarily cytosolic. Thus, the primary role of Prom1 in the human RPE is not structural, and there are differences in spatiotemporal expression and localization of Prom1 between in vitro cultures and in vivo tissue sections. Since Prom1 mutations cause dominant macular degeneration in humans,[14,52] incomplete understanding of the multiple pathways that cooperate in Prom1 expression and localization combined with the complex pathogenesis of retinal disorders pose significant challenges for developing new therapies. Thus, additional studies are necessary to address the physiological impact of these differences in Prom1 localization and understand the ever-expanding functional diversity of Prom1 outside photoreceptor cell biology. Our localization studies demonstrate the presence of Prom1 in the perinuclear region reminiscent of the endoplasmic reticulum (ER), Golgi, and trans Golgi network. Since Prom1 is an integral membrane protein in most cell types but primarily present in the cytoplasm in RPE cells, it is likely that Prom1 is an essential component of the intracellular membrane-enclosed organelles, including ER and Golgi bodies. Several models have attempted to explain the subcellular localization of proteins, including mono and poly-ubiquitination of proteins. Since ubiquitination of Prom1 has been reported,[59] it is attractive to speculate that ubiquitination regulates cytoplasmic localization of Prom1 in the RPE. A recent study showed that Prom1 was dynamically released from plasma membrane into cytoplasm in response to high glucose,[12] raising the possibility of Prom1's cytoplasmic accumulation by its trafficking from the cell surface. However, only few studies have reported the intracellular localization of Prom1 in addition to its cell surface expression.[60,61]

To elucidate the role of Prom1 in the RPE, we performed a series of studies using overexpression and genomic editing strategies. These studies were aimed at spatiotemporal modulation of Prom1 expression, which could impact RPE function. Lentiviral overexpression of Prom1 potentiated expression of autophagy markers Atg5, Atg7, decreased p62 accumulation, and constitutively activated autophagy. Furthermore, overexpression of Prom1 resulted in the expression of the same splice variant 3, which is endogenously expressed in ARPE-19 cells, demonstrating that our observations are focused on one splice variant of Prom1 and its function. To rule out the involvement of other possible Prom1 splice variants in the regulation of autophagy in ARPE-19 cells, we used CRISPR/Cas9-mediated genome editing, which is capable of deleting all splice variants. Genomic deletion of Prom1 blocked basal Atg5, Atg7 expression, increased p62 expression, and, consequently inhibited basal autophagy flux, reinforcing the concept that Prom1 is a central regulator of autophagy in vitro in ARPE-19 cells. It is unclear how Prom1 regulates the expression of Atg5 and Atg7 in the RPE and warrants further investigation. The RPE layer is well preserved in 1-month-old Prom1$^{-/-}$ mouse

Investigative Ophthalmology & Visual Science

retina with intact microvilli and basal infoldings.[8] However, by 6 months, a loss of RPE pigmentation with morphological alterations were observed in the Prom1$^{-/-}$ retinas, demonstrating that Prom1 is not required for retinal development but is rather necessary for maintaining retinal homeostasis. Our data support the hypothesis that this role is performed through the regulation of autophagy.

Prom1-dependent autophagy has recently been recognized to be an important contributor of cancer stem cell survival and resistance of cancer cells to anticancer therapies.[62] There is growing evidence that increased autophagic flux in CD133^{+} cancer stem cells contributes to treatment failure and tumor relapse. Since hypoxic microenvironments tightly regulate the inherent properties of cancer stem cells,[63] the survival of stem cells in this microenvironment is dependent on prosurvival mechanisms involving autophagy. A recent study showed that Prom1/CD133^{+} cancer stem cells in a hypoxic environment formed more autophagic puncta and contained higher levels of LC3-II compared to Prom1/CD133^{-} cells.[12] Chemotherapy further increased autophagy without causing the death of CD133^{+} cells. Interestingly, inhibition of autophagy in cancer stem cells either by pharmacologic intervention or Atg gene silencing increased sensitivity to chemotherapy-mediated cytotoxicity.[62] Thus, the relationship we have demonstrated between Prom1 and autophagy in the RPE may also be the mechanism that confers protection against chemotherapy and radiotherapy in Prom1/CD133^{+} cancer stem cells. Furthermore, Prom1 trafficking in response to changes in cell microenvironment such as low glucose and hypoxia caused release of membrane bound Prom1 to the cytoplasm,[12] which promoted autophagy in cancer cells, suggesting that dynamic alteration of CD133 localization from membranes to the cytosol in response to diverse environmental cues is necessary for the induction of autophagy to increase cell survival. In hepatoma cells, expression of Prom1/CD133 promoted autophagosome formation, and silencing of Prom1 attenuated this activity further confirming that Prom1 is an essential component of the autophagic machinery.[12] In agreement with this conclusion, our own data show that exposure of RPE cells overexpressing Prom1 conferred cytoprotection from Nutlin-3-induced cell death due to increased autophagic flux. Thus, Prom1-mediated autophagy may play a novel role in mediating survival of diverse cell types, including cancer stems cells.

Hypoxia, nutrient deprivation, and ER stress upregulate autophagy, an adaptive housekeeping mechanism that promotes organismal health and counteracts the aging process.[64,65] Cells exposed to stressors utilize various strategies including autophagy to avoid cell death and overcome nutritional deficiency.[66] Because aging increased Prom1 expression and genetic deletion of Prom1 abrogated autophagosome maturation and basal autophagy in primary RPE cultures, we examined whether exposure of RPE cells to various stressors including hypoxia and nutrient deprivation triggered autophagic activity with concomitant upregulation of Prom1 expression. Relative hypoxia increased autophagy protein Atg5 and decreased p62 expression with concomitant reduction of its phosphorylation at Ser349, indicating robust activation of autophagy flux. It is noteworthy that induction of autophagy was coupled with increased Prom1 expression after prolonged exposure to hypoxia, suggesting that Prom1 protects the RPE against prolonged hypoxia by upregulation of autophagy. Exposure of RPE cells to EBSS medium rapidly activated autophagy. More importantly, EBSS-mediated induction of autophagy is correlated with increased expression of Prom1, suggesting that nutrient deprivation-induced autophagosome formation requires the engagement of Prom1. Mechanistically, mTOR is a central signaling pathway that coordinates the cellular processes with metabolic homeostasis through its ability to negatively regulate autophagy. Both nutrient deprivation and hypoxia rapidly inactivated mTORC1. These stress signals had a similar effect on mTORC2 inhibition. Together, these results suggest a model in which increased Prom1 expression and mTORC1/mTORC2 inhibition orchestrate the induction of autophagy flux in response to stress signals in the RPE (Fig. 12).

We analyzed the mechanisms through which Prom1 regulates autophagy. Although mTORC1 and mTORC2 are independent regulators of autophagy, mTORC2 can both positively and negatively regulate autophagy.[67] Overexpression of Prom1 inhibited mTORC1 and mTORC2 signaling and, thereby, activated basal autophagy flux. Bafilomycin failed to accumulate p62 in cells overexpressing Prom1 strongly suggesting rapid turnover of LC3-I to LC3-II. Exposure of cells overexpressing Prom1 to autophagy modulating drugs confirmed potentiation of autophagy flux and was further accompanied by complete inhibition of mTORC1/2 signaling. The importance of this process was verified in Prom1 KO cells that showed increased activation of mTORC1 and mTORC2. These cells also exhibited reduced LC3 puncta formation and decreased trafficking of autophagosomes with lysosomes, suggesting that Prom1 plays important upstream and downstream roles in autophagy and cellular homeostasis in the RPE. It is intriguing to note that mTOR inhibitors and amino-acid starvation abolished mTORC1 and mTORC2 activation in KO cells but failed to restore autophagy, confirming that inhibition of mTORC1/2 is necessary but insufficient in the regulation of Prom1-dependent autophagy. These observations further indicate that Prom1-mediated upstream suppression of mTOR is mechanistically linked to downstream events in the autophagy pathway. For the first time, we show that the Prom1 protein is a partner of a macromolecular complex involving p62 and cytosolic HDAC6, both of which are integral components of autophagosome formation and trafficking of the autophagosomes to the lysosomes. Although several complex molecular mechanisms including Rab7,[68] endosomal-sorting,[69] lysosomal V-ATPase,[70] mTORC1,[71] and post-translational modifications of tubulin[72] have also been implicated in the autophagosome-lysosome fusion, our own data show that Prom1 participates in delivery of the autophagosomal cargo to the lysosomes in the RPE through its downstream interaction with p62 and HDAC6.

Based on our work, we propose a conceptual model in which Prom1-dependent negative regulation of mTORC1/2 and a Prom1-interacting macromolecular signaling complex direct autophagosome biogenesis in the RPE (Fig. 12). Several experimental approaches including relative hypoxia, nutrient deprivation, and ectopic overexpression demonstrate a significant correlation between Prom1 expression and induction of autophagy. Increased Prom1 expression led to upstream inhibition of both mTORC1 and mTORC2. Although it is unknown how Prom1 negatively regulates mTOR signaling in the RPE, previous studies demonstrated that inhibition of mTOR signaling increased the CD133^{+} subpopulations in vitro and in vivo, whereas activation of mTOR by Rheb significantly decreased CD133 expression.[73] In cancer cells, a mechanistic relationship exists between CD133 and the hypoxia-inducible factor-1α, a downstream target in the mTOR signaling pathway.[74] These previous observations support the presence of a molecular cross talk between Prom1 and mTOR signaling in the regulation of autophagy flux in the RPE. Furthermore, our data demonstrate that Prom1 was an essential component of a downstream signaling complex involving p62 and HDAC6, which triggered autophagosome maturation and enhanced cycling of autophagosomes with lysosomes. KO of Prom1 increased mTORC1 and mTORC2 activities and decreased the recruitment of p62 to the macromolecular complex. These

Investigative Ophthalmology & Visual Science

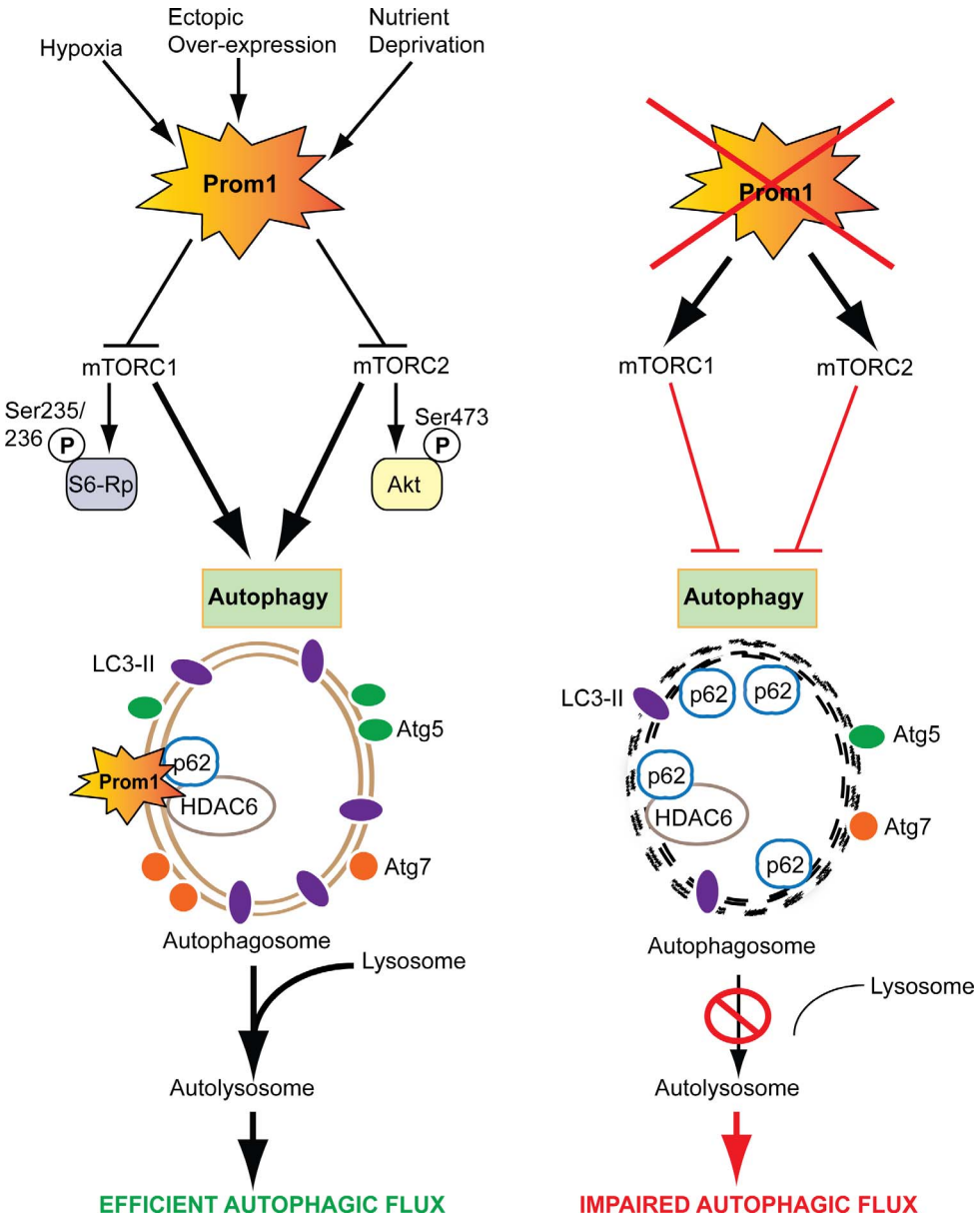

Figure 12. Schematic showing the molecular mechanisms regulating Prom1-dependent autophagy in the RPE. Relative hypoxia (using 8% O_2), nutrient deprivation (using EBSS), and ectopic overexpression of Prom1 (using WT lentivirus) increase Prom1 expression in the RPE with concomitant upstream inhibition of mTORC1 (decreased levels of phospho-S6 Ribosomal protein Ser235/236) and mTORC2 (decreased levels of Akt Ser473). Increased expression of Prom1 was associated with higher levels of Atg5, Atg7, and LC3-II/LC3-I ratio. Prom1 formed a macromolecular complex with p62 and HDAC6, increased autophagosome maturation, enhanced cycling of autophagosomes with lysosomes, and, consequently, increased autophagic flux in the RPE. KO of Prom1 imposes a double lock in the autophagy pathway, first activating mTORC1 and mTORC2 and then inhibiting the maturation and trafficking of autophagosomes through disruption of the macromolecular complex with p62 and HDAC6. Together, these molecular mechanisms demonstrate that Prom1 is an essential component of the autophagy pathway in the RPE.

molecular events increased p62 accumulation, impaired autophagosome maturation, and autophagy flux. Together, our results demonstrate that Prom1 is a key regulator of autophagy in the RPE. Modulation of its age-related expression may represent a cellular mechanism that protects the cell from age-related decline in autophagy flux, a critical role played by the RPE. It is interesting to speculate that such a decline in cellular homeostasis may play a mechanistic role in the AMD phenotype and Stargardt-like (STGD4) macular dystrophy disease. In addition, the newly defined role for Prom1 in autophagy may explain the resistance of $CD133^+$ cancer cells to hypoxia and chemotherapy.

Acknowledgments

The authors thank the Mid South Eye Bank for providing postmortem human donor eyes of various ages, Richard Demarco (EMD Millipore Corp., Billerica, MA, USA) for assistance with Amnis flow cytometry, and Weihong Huo for technical assistance.

Supported by a Shulsky Foundation research grant, an unrestricted departmental grant from Research to Prevent Blindness (New York, NY, USA), the Plough Foundation (Memphis, TN, USA), the Lions of Arkansas, and the NEI vision core Grant PHS 3P30 EY013080. The authors alone are responsible for the content and writing of the paper.

Disclosure: **S. Bhattacharya**, None; **J. Yin**, None; **C.S. Winborn**, None; **Q. Zhang**, None; **J. Yue**, None; **E. Chaum**, None

References

1. Jaszai J, Fargeas CA, Florek M, Huttner WB, Corbeil D. Focus on molecules: prominin-1 (CD133). *Exp Eye Res*. 2007;85: 585–586.
2. Miraglia S, Godfrey W, Yin AH, et al. A novel five-transmembrane hematopoietic stem cell antigen: isolation, characterization, and molecular cloning. *Blood*. 1997;90: 5013–5021.
3. Yin AH, Miraglia S, Zanjani ED, et al. AC133, a novel marker for human hematopoietic stem and progenitor cells. *Blood*. 1997;90:5002–5012.
4. Fargeas CA, Fonseca AV, Huttner WB, Corbeil D. Prominin-1 (CD133): from progenitor cells to human diseases. *Future Lipidology*. 2006;1:213–225.
5. Snippert HJ, van Es JH, van den Born M, et al. Prominin-1/CD133 marks stem cells and early progenitors in mouse small intestine. *Gastroenterology*. 2009;136:2187–2194.
6. Corbeil D, Roper K, Fargeas CA, Joester A, Huttner WB. Prominin: a story of cholesterol, plasma membrane protrusions and human pathology. *Traffic*. 2001;2:82–91.
7. Pine SR, Ryan BM, Varticovski L, Robles AI, Harris CC. Microenvironmental modulation of asymmetric cell division in human lung cancer cells. *Proc Natl Acad Sci U S A*. 2010; 107:2195–2200.
8. Zacchigna S, Oh H, Wilsch-Brauninger M, et al. Loss of the cholesterol-binding protein prominin-1/CD133 causes disk dysmorphogenesis and photoreceptor degeneration. *J Neurosci*. 2009;29:2297–2308.
9. Janich P, Corbeil D. GM1 and GM3 gangliosides highlight distinct lipid microdomains within the apical domain of epithelial cells. *FEBS Lett*. 2007;581:1783–1787.
10. Roper K, Corbeil D, Huttner WB. Retention of prominin in microvilli reveals distinct cholesterol-based lipid microdomains in the apical plasma membrane. *Nat Cell Biol*. 2000;2:582–592.
11. Weigmann A, Corbeil D, Hellwig A, Huttner WB. Prominin, a novel microvilli-specific polytopic membrane protein of the apical surface of epithelial cells, is targeted to plasmalemmal protrusions of non-epithelial cells. *Proc Natl Acad Sci U S A*. 1997;94:12425–12430.
12. Chen H, Luo Z, Dong L, et al. CD133/prominin-1-mediated autophagy and glucose uptake beneficial for hepatoma cell survival. *PLoS One*. 2013;8:e56878.
13. Mak AB, Nixon AM, Kittanakom S, et al. Regulation of CD133 by HDAC6 promotes beta-catenin signaling to suppress cancer cell differentiation. *Cell Reports*. 2012;2:951–963.
14. Yang Z, Chen Y, Lillo C, et al. Mutant prominin 1 found in patients with macular degeneration disrupts photoreceptor disk morphogenesis in mice. *J Clin Invest*. 2008;118:2908–2916.
15. Fargeas CA, Buttner E, Corbeil D. Commentary: prom1 function in development, intestinal inflammation, and intestinal tumorigenesis. *Front Oncol*. 2015;5:91.
16. Michaelides M, Johnson S, Poulson A, et al. An autosomal dominant bull's-eye macular dystrophy (MCDR2) that maps to the short arm of chromosome 4. *Invest Ophthalmol Vis Sci*. 2003;44:1657–1662.
17. Zhang Q, Zulfiqar F, Xiao X, et al. Severe retinitis pigmentosa mapped to 4p15 and associated with a novel mutation in the PROM1 gene. *Hum Genet*. 2007;122:293–299.
18. Bok D. The retinal pigment epithelium: a versatile partner in vision. *J Cell Sci Suppl*. 1993;17:189–195.
19. Frost LS, Mitchell CH, Boesze-Battaglia K. Autophagy in the eye: implications for ocular cell health. *Exp Eye Res*. 2014; 124:56–66.
20. Kim JY, Zhao H, Martinez J, et al. Noncanonical autophagy promotes the visual cycle. *Cell*. 2013;154:365–376.
21. Cuervo AM, Wong E. Chaperone-mediated autophagy: roles in disease and aging. *Cell Res*. 2014;24:92–104.
22. Seo SJ, Krebs MP, Mao H, Jones K, Conners M, Lewin AS. Pathological consequences of long-term mitochondrial oxidative stress in the mouse retinal pigment epithelium. *Exp Eye Res*. 2012;101:60–71.
23. Johansen T, Lamark T. Selective autophagy mediated by autophagic adapter proteins. *Autophagy*. 2011;7:279–296.
24. Laplante M, Sabatini DM. mTOR signaling in growth control and disease. *Cell*. 2012;149:274–293.
25. Kim J, Kundu M, Viollet B, Guan KL. AMPK and mTOR regulate autophagy through direct phosphorylation of Ulk1. *Nat Cell Biol*. 2011;13:132–141.
26. Sarbassov DD, Guertin DA, Ali SM, Sabatini DM. Phosphorylation and regulation of Akt/PKB by the rictor-mTOR complex. *Science*. 2005;307:1098–1101.
27. Mitter SK, Song C, Qi X, et al. Dysregulated autophagy in the RPE is associated with increased susceptibility to oxidative stress and AMD. *Autophagy*. 2014;10:1989–2005.
28. Zhao C, Yasumura D, Li X, et al. mTOR-mediated dedifferentiation of the retinal pigment epithelium initiates photoreceptor degeneration in mice. *J Clin Invest*. 2011;121:369–383.
29. Nixon RA. The role of autophagy in neurodegenerative disease. *Nat Med*. 2013;19:983–997.
30. Yue J, Sheng Y, Ren A, Penmatsa S. A miR-21 hairpin structure-based gene knockdown vector. *Biochem Biophys Res Commun*. 2010;394:667–672.
31. Chaum E, Yin J, Yang H, Thomas F, Lang JC. Quantitative AP-1 gene regulation by oxidative stress in the human retinal pigment epithelium. *J Cell Biochem*. 2009;108:1280–1291.
32. Bhattacharya S, Ray RM, Chaum E, Johnson DA, Johnson LR. Inhibition of Mdm2 sensitizes human retinal pigment epithelial cells to apoptosis. *Invest Ophthalmol Vis Sci*. 2011;52:3368–3380.
33. Zhu D, Deng X, Spee C, et al. Polarized secretion of PEDF from human embryonic stem cell-derived RPE promotes retinal progenitor cell survival. *Invest Ophthalmol Vis Sci*. 2011;52:1573–1585.
34. Bhattacharya S, Chaum E, Johnson DA, Johnson LR. Age-related susceptibility to apoptosis in human retinal pigment epithelial cells is triggered by disruption of p53-Mdm2 association. *Invest Ophthalmol Vis Sci*. 2012;53:8350–8366.
35. Mizushima N. Autophagy: process and function. *Genes Dev*. 2007;21:2861–2873.
36. Loos B, du Toit A, Hofmeyr JH. Defining and measuring autophagosome flux-concept and reality. *Autophagy*. 2014; 10:2087–2096.
37. Fang Y, Tan J, Zhang Q. Signaling pathways and mechanisms of hypoxia-induced autophagy in the animal cells. *Cell Biol Int*. 2015;39:891–898.
38. Forooghian F, Razavi R, Timms L. Hypoxia-inducible factor expression in human RPE cells. *Br J Ophthalmol*. 2007;91: 1406–1410.
39. Vadlapatla RK, Vadlapudi AD, Pal D, Mukherji M, Mitra AK. Ritonavir inhibits HIF-1alpha-mediated VEGF expression in retinal pigment epithelial cells in vitro. *Eye (Lond)*. 2014;28: 93–101.
40. Carreau A, El Hafny-Rahbi B, Matejuk A, Grillon C, Kieda C. Why is the partial oxygen pressure of human tissues a crucial parameter? Small molecules and hypoxia. *J Cell Mol Med*. 2011;15:1239–1253.

Investigative Ophthalmology & Visual Science

41. Mintun MA, Lundstrom BN, Snyder AZ, Vlassenko AG, Shulman GL, Raichle ME. Blood flow and oxygen delivery to human brain during functional activity: theoretical modeling and experimental data. *Proc Natl Acad Sci U S A*. 2001;98:6859–6864.
42. Klionsky DJ, Abdelmohsen K, Abe A, et al. Guidelines for the use and interpretation of assays for monitoring autophagy (3rd edition). *Autophagy*. 2016;12:1–222.
43. Mizushima N, Yamamoto A, Matsui M, Yoshimori T, Ohsumi Y. In vivo analysis of autophagy in response to nutrient starvation using transgenic mice expressing a fluorescent autophagosome marker. *Mol Biol Cell*. 2004;15:1101–1111.
44. Wang AL, Boulton ME, Dunn WA Jr, et al. Using LC3 to monitor autophagy flux in the retinal pigment epithelium. *Autophagy*. 2009;5:1190–1193.
45. Yamamoto A, Tagawa Y, Yoshimori T, Moriyama Y, Masaki R, Tashiro Y. Bafilomycin A1 prevents maturation of autophagic vacuoles by inhibiting fusion between autophagosomes and lysosomes in rat hepatoma cell line, H-4-II-E cells. *Cell Struct Funct*. 1998;23:33–42.
46. Bjorkoy G, Lamark T, Pankiv S, Overvatn A, Brech A, Johansen T. Monitoring autophagic degradation of p62/SQSTM1. *Methods Enzymol*. 2009;452:181–197.
47. Acosta-Jaquez HA, Keller JA, Foster KG, et al. Site-specific mTOR phosphorylation promotes mTORC1-mediated signaling and cell growth. *Mol Cell Biol*. 2009;29:4308–4324.
48. Meyuhas O. Ribosomal protein S6 phosphorylation: four decades of research. *Int Rev Cell Mol Biol*. 2015;320:41–73.
49. Castino R, Lazzeri G, Lenzi P, et al. Suppression of autophagy precipitates neuronal cell death following low doses of methamphetamine. *J Neurochem*. 2008;106:1426–1439.
50. Wang T, Lao U, Edgar BA. TOR-mediated autophagy regulates cell death in Drosophila neurodegenerative disease. *J Cell Biol*. 2009;186:703–711.
51. Shintani T, Klionsky DJ. Autophagy in health and disease: a double-edged sword. *Science*. 2004;306:990–995.
52. Permanyer J, Navarro R, Friedman J, et al. Autosomal recessive retinitis pigmentosa with early macular affectation caused by premature truncation in PROM1. *Invest Ophthalmol Vis Sci*. 2010;51:2656–2663.
53. Feldman ME, Apsel B, Uotila A, et al. Active-site inhibitors of mTOR target rapamycin-resistant outputs of mTORC1 and mTORC2. *PLoS Biol*. 2009;7:e38.
54. Thoreen CC, Kang SA, Chang JW, et al. An ATP-competitive mammalian target of rapamycin inhibitor reveals rapamycin-resistant functions of mTORC1. *J Biol Chem*. 2009;284:8023–8032.
55. Shalem O, Sanjana NE, Hartenian E, et al. Genome-scale CRISPR-Cas9 knockout screening in human cells. *Science*. 2014;343:84–87.
56. Marzesco AM. Prominin-1-containing membrane vesicles: origins, formation, and utility. *Adv Exp Med Biol*. 2013;777:41–54.
57. Fargeas CA, Florek M, Huttner WB, Corbeil D. Characterization of prominin-2, a new member of the prominin family of pentaspan membrane glycoproteins. *J Biol Chem*. 2003;278:8586–8596.
58. Harris JR, Fisher R, Jorgensen M, Kaushal S, Scott EW. CD133 progenitor cells from the bone marrow contribute to retinal pigment epithelium repair. *Stem Cells*. 2009;27:457–466.
59. Karbanova J, Laco J, Marzesco AM, et al. Human prominin-1 (CD133) is detected in both neoplastic and non-neoplastic salivary gland diseases and released into saliva in a ubiquitinated form. *PLoS One*. 2014;9:e98927.
60. Nunukova A, Neradil J, Skoda J, et al. Atypical nuclear localization of CD133 plasma membrane glycoprotein in rhabdomyosarcoma cell lines. *Int J Mol Med*. 2015;36:65–72.
61. Huang M, Zhu H, Feng J, Ni S, Huang J. High CD133 expression in the nucleus and cytoplasm predicts poor prognosis in non-small cell lung cancer. *Dis Markers*. 2015;2015:986095.
62. Wei MF, Chen MW, Chen KC, et al. Autophagy promotes resistance to photodynamic therapy-induced apoptosis selectively in colorectal cancer stem-like cells. *Autophagy*. 2014;10:1179–1192.
63. Jin S, White E. Role of autophagy in cancer: management of metabolic stress. *Autophagy*. 2007;3:28–31.
64. Altman BJ, Rathmell JC. Metabolic stress in autophagy and cell death pathways. *Cold Spring Harb Perspect Biol*. 2012;4:a008763.
65. Levine B, Kroemer G. Autophagy in aging, disease and death: the true identity of a cell death impostor. *Cell Death Differ*. 2009;16:1–2.
66. Ojha R, Bhattacharyya S, Singh SK. Autophagy in cancer stem cells: a potential link between chemoresistance, recurrence, and metastasis. *Biores Open Access*. 2015;4:97–108.
67. Fan QW, Cheng C, Hackett C, et al. Akt and autophagy cooperate to promote survival of drug-resistant glioma. *Science Signaling*. 2010;3:ra81.
68. Jager S, Bucci C, Tanida I, et al. Role for Rab7 in maturation of late autophagic vacuoles. *J Cell Sci*. 2004;117:4837–4848.
69. Henne WM, Buchkovich NJ, Emr SD. The ESCRT pathway. *Dev Cell*. 2011;21:77–91.
70. Williamson WR, Wang D, Haberman AS, Hiesinger PR. A dual function of V0-ATPase a1 provides an endolysosomal degradation mechanism in Drosophila melanogaster photoreceptors. *J Cell Biol*. 2010;189:885–899.
71. Zhou J, Tan SH, Nicolas V, et al. Activation of lysosomal function in the course of autophagy via mTORC1 suppression and autophagosome-lysosome fusion. *Cell Res*. 2013;23:508–523.
72. Toops KA, Tan LX, Jiang Z, Radu RA, Lakkaraju A. Cholesterol-mediated activation of acid sphingomyelinase disrupts autophagy in the retinal pigment epithelium. *Mol Biol Cell*. 2015;26:1–14.
73. Yang Z, Zhang L, Ma A, et al. Transient mTOR inhibition facilitates continuous growth of liver tumors by modulating the maintenance of CD133+ cell populations. *PLoS One*. 2011;6:e28405.
74. Matsumoto K, Arao T, Tanaka K, et al. mTOR signal and hypoxia-inducible factor-1 alpha regulate CD133 expression in cancer cells. *Cancer Res*. 2009;69:7160–7164.

Investigative Ophthalmology & Visual Science